AD-A111 222   HEBREW UNIV JERUSALEM (ISRAEL)   F/G 7/4
               THE DYNAMICS OF NONSPHERICAL PARTICLES. V. THE WALL EFFECT IN O--ETC(U)
               NOV 81 I GALLILY   DA-ERO-78-G-057
UNCLASSIFIED   NL

| OF |
AD A
111222

END
DATE
FILMED
103-82
DTIC

THE DYNAMICS OF NONSPHERICAL PARTICLES.

V. THE WALL EFFECT IN ORDERLY
DEPOSITION; BROWNIAN DIFFUSION

by

Isaiah Gallily

December 1981

The Hebrew University of Jerusalem, Jerusalem,Israel

FEB 2 1982

E

THE DYNAMICS OF NONSPHERICAL PARTICLES

V. THE WALL EFFECT IN ORDERLY
DEPOSITION; BROWNIAN DIFFUSION

by

Isaiah Gallily

December 1981

The Hebrew University of Jerusalem, Jerusalem,Israel

REPORT DOCUMENTATION PAGE	READ INSTRUCTIONS BEFORE COMPLETING FORM

1. REPORT NUMBER	2. GOVT ACCESSION NO. *AD-A111222*	3. RECIPIENT'S CATALOG NUMBER

4. TITLE (and Subtitle) Dynamics of Nonspherical Aerosol Particles	5. TYPE OF REPORT & PERIOD COVERED Final Technical Report Mar 78 – Oct 81
	6. PERFORMING ORG. REPORT NUMBER

7. AUTHOR(s) Prof. Isaiah Gallily	8. CONTRACT OR GRANT NUMBER(s) DAERO-78-G-057

9. PERFORMING ORGANIZATION NAME AND ADDRESS Department of Atmospheric Sciences The Hebrew University of Jerusalem Jerusalem, Israel	10. PROGRAM ELEMENT, PROJECT, TASK AREA & WORK UNIT NUMBERS 61102A IT161102BH57-01

11. CONTROLLING OFFICE NAME AND ADDRESS USARDSG-UK Box 65, FPO New York, NY 09510	12. REPORT DATE Nov 1981
	13. NUMBER OF PAGES

14. MONITORING AGENCY NAME & ADDRESS(if different from Controlling Office)	15. SECURITY CLASS. (of this report) Unclassified
	15a. DECLASSIFICATION/DOWNGRADING SCHEDULE

16. DISTRIBUTION STATEMENT (of this Report)

Approved for Public Release; Distribution Unlimited

17. DISTRIBUTION STATEMENT (of the abstract entered in Block 20, if different from Report)

18. SUPPLEMENTARY NOTES

None

19. KEY WORDS (Continue on reverse side if necessary and identify by block number)

20. ABSTRACT (Continue on reverse side if necessary and identify by block number)

The effect of the wall on the motion of elongated aerosol particles was calculated on the basis of the (powerful) slender body theory for a quiet and flowing medium. The cases treated were those of cylindrical particles moving in a quiet environment or a Couette or a Poiseuille flow near plannar surfaces with various inclinations to the horizontal.

DD FORM 1473 EDITION OF 1 NOV 65 IS OBSOLETE
S/N 0102-LF-014-6601

Experiments of trajectory photographing were performed in a liquid-tank under creeping flow conditions and typical (aerosol)Reynolds numbers whereby very good correspondence with computations was obtained.

The Brownian diffusion of (very small) cylindrical or discoidal aerosol particles was also studied while being based on Brennners' formal structure. To evaluate the significant orientation density function, the (mid-diameter) rotational diffusion coefficient of the particles was calculated by a statistical-mechanical method. The values of the coefficients were found to be larger than those computed on the basis of continuum theory by a factor of about 30.

The typical diffusion situation of deposition on a plane within a quiet air was treated.

Accession For

NTIS

U

J

D

A

ABSTRACT

The effect of the wall on the motion of elongated aerosol particles was calculated on the basis of the(powerful) slender body theory for a quiet and flowing medium. The cases treated were those of cylindrical particles moving in a quiet environment or a Couette or a Poiseuille flow near plannar surfaces with various inclinations to the horizontal.

Experiments of trajectory photographing were performed in a liquid-tank under creeping flow conditions and typical (aerosol) Reynolds numbers whereby very good correspondence with computations was obtained.

The Brownian diffusion of (very small) cylindrical or discoidal aerosol particles was also studied while being based on Brenners' formal structure. To evaluate the signficant orientation density function, the (mid-diameter)rotational diffusion coefficient of the particles was calculated by a statistical-mechanical method. The values of the coefficients were found to be larger than those computed on the basis of continuum theory by a factor of about 30.

The typical diffusion situation of deposition on a plane within a quiet air was treated.

TABLE OF CONTENTS

Page

INTRODUCTION

During the past several years a series of studies on the transport mechanics of non-spherical aerosol particles was carried out mostly with the support of the European Research Office, U.S. Army. These studies were summarized in the final reports:

The Dynamics of Nonspherical Particles

I. Controlled Generation of Nonspherical Aerosols and Methods for Their Size, Concentration and Electric Size Measurement (Contract DAJA 37-72-3875; 1974).

II. Mobility in Non-Orienting Fields (Contract DAJA 37-74-C-1208; 1975).

III. Mobility and Deposition in Still Air (Contract DAERO-75-G-021; 1977).

IV. Deposition from Flow (Contract DAERO-76-G-014; 1978)

and in the parallel journal publications:

1. "On the stochastic Motion of Nonspherical Aerosol Particles. I. The Aerodynamic Radius Concept" by Isaiah Gallily and Aaron Hi-Cohen, J. Colloid Interface Sci. 56, 443-59 (1976)

2. "_____, II. The Overall Drift Angle in Sedimentation", by Matitia A. Weiss, Aaron-Hi Cohen and Isaiah Gallily, J. Aerosol Sci. 9, 527-41 (1978).

3. "On the Orderly Nature of the Motion of Nonspherical Aerosol Particles. I. Deposition from a Laminar Flow." by Isaiah Gallily and Alferd D. Eisner, J. Colloid interface Sci. 68, 326-37 (1979).

Likewise, they were reported in the following articles:

4, "On the Orderly Nature of the Motion of Nonspherical Aerosol

Particles. II. Inertial Collision between a Spherical Large Drop-

let and an Axially Symmetrical Elongated Particle" by Isaiah Gallily

and Aaron-Hi Cohe, J. Colloid Interface Sci. 68, 338-56 (1979).

5. "_____,II._____, Further Results," by Isaiah Gallily and

Aaron Hi-Cohen, ibid. 71, 628-30 (1979).

The efforts invested in all of these investigations culminated in the

establishment of a method of claculation of the gravitational sedimentation

in still and laminarily flowing gas, and of the inertial impaction on

various surfaces of axi-symmetrical particles such as cylinders and

disks. The method has been ellaborated in the (above) publications 1-5 and

partially checked by experiments; however, it is far from being complete.

One problem in the analysis of our particles' transfer phenomena which

has not been considered is the effect of the surface exposed to the aerosol on

the collection process itself. The effect, related here only to the motion

of the particles in the adjoining gas layer, is due to :

    a. The fluiddynamic interaction between a particle approaching a

surface and the latter which essentially stems from the change of the flow field

due to the emergence of an additional boundary condition.

    b. The presence of long (electrostatic) or short (Van der Waals) surface

particle forces.

Another untreated problem concerns the stochastic diffusional turbulent and/or

Brownian movement of the particles.

It is needless to stress the significance of the first problem which has been treated scarcely for the case of spherical particles by Brenner(1), Gallily and Mahrer (2) and others and has been almost untouched in the case of the nonspherical ones.

In most studies on the orderly motion of any particle, expressed by the equation of translation

$$m \, d\mathbf{u} / dt = \sum_i \mathbf{F}_{e,i} + \mathbf{F}_F \qquad [1]$$

and rotation

$$d(\mathbf{I}^* \cdot \boldsymbol{\omega})/dt = \sum_i \mathbf{L}_{e,i} + \mathbf{L}_F \qquad [2]$$

the fluiddynamic operating force $\mathbf{F}_F$ and torque $\mathbf{L}_F$ have been calculated for the substitute situation in which the particle is infinitely far from the (collecting) surface. This has been obviously a simplification whose justification was checked in the calculation of $\mathbf{F}_F$ and $\mathbf{L}_F$ for some spherical cases (1,2). For the nonspherical case, it has not been studied at all.

The importance of the second problem is self evident for sufficiently turbulent field or very small particles for which the fluctuating part of the force $\mathbf{F}_F$, viz. $\mathbf{F}_F - \langle \mathbf{F}_F \rangle$, can not be neglected in comparison with the mean one $\langle \mathbf{F}_F \rangle$.

AIM OF STUDY

In view of the above review of the state of research, it was thought
worthwhile to investigate:

1. The effect of the collecting surface on the motion of nonsphe-
rical particles near, and their deposition on it, and, independently,

2. The diffusion of nonspherical particles.

These two problems seemed immediately too formidable for a general
treatment; thus their study was restricted in the first subject to the
case of cylindrical particles much larger than the mean free path $\bar{l}$ of
the medium's molecules ($Kn \ll 1$), and a planar solid wall, and
in the second subject to the Brownian diffusion of cylindrical and discoidal
particles much smaller than $\bar{l}$ ($Kn \ll 1$) . Cylindrical and
discoidal forms respectively serve as idealized model shapes of the
real (harmful)asbestos or other significant fibrous particles and of
platelet-like ones. So, the restriction to the above morphology is not
very limiting in significance.

A. THE WALL EFFECT

I. Theoretical

1. Method

a. General

Here we preferred to use slender body theory rather than the (limited)
method of Wakiya which is based on Fourier analysis technique (3).

The slender body theory method is much more general than the latter; it can be employed in situations where the (aerosol) particle is even far from walls with a better advantage than that obtained by being based on the much used Oberbeck's (4) and Jeffery's (5) equations. In other words, it is very useful.

The method is apt for the treatment of the motion of particles whose characteristic size r_c $(= \sqrt{S / 4\pi})^1$ is much larger than the mean free path $\bar{l}$ of the medium's molecules $(Kn = \frac{\bar{l}}{r_c} \gg 1$ and whose characteristic Reynolds number Re is much smaller than unity. In fhat case, the equations of fluid motion to be solved are

$$\mu \nabla^2 \mathbf{v}(\mathbf{r}) - \nabla p = 0 \qquad\qquad [3]$$

and

$$\nabla \cdot \mathbf{v}(\mathbf{r}) = 0 \qquad . \qquad\qquad [4]$$

The theory, developed by Batchelor (6), Chwang and Wu(7), Blake (8), Cox (9) and others, deals with elongated particles in which the ratio k between the characteristic cross-sectional radius b and the semi-length l is $k = \frac{b}{l} \ll 1$, the change of the local equivalent cross-sectional

---

[1] For symbols see NOMENCLATURE

radius $\mathring{}_{r'}$ is small compared with $\mathring{}_{r'}/\mathring{}$, and the local radius of curvature is much greater than $\mathring{}$ (Fig. 1).
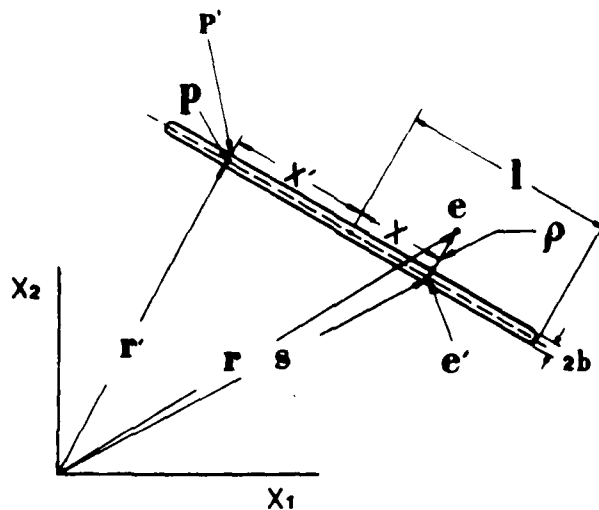

Fig. 1. A slender body (not necessarily a straight cylinder); coordinates used in the analysis.

Under these conditions, the disturbance velocity $\mathbf{v}(\mathbf{r})$ produced by the moving particle is given by the multipole expansion

$$v_i(r) = \int_{-\ell}^{\ell} f_j(r')\, u_{ij}(r, r')\, dr' + \int_{-\ell}^{\ell} f_{jk}(r')\, u_{ijk}(r, r')\, dr'$$

$$+ \int f_{jk\lambda}(r')\, u_{ijk\lambda}(r, r')\, dr' + \ldots \tag{5}$$

where, with the Einstein's convention adhered to, $f_j(r')$ (Stokeslet),
$f_{jk}(r')$ (doublet), $f_{jk\lambda}(r')$ etc. are
(imaginary) poles causing the disturbances $u_{ij}(r, r')$ etc.; the latter
are actually the proper Green functions (APPENDIX 1).

The calculation of the (critically required) fluiddynamic force F_F
and torque L_F appearing in Eqs. [1] and [2] can be performed
once the Stokelet $f_j(r')$ distribution is known since (Fig.1)

$$F_F = \int_{-\ell}^{\ell} f(s)\, ds \tag{6}$$

and

$$L_F = \int_{-\ell}^{\ell} (x \times f(s))\, ds \tag{7}$$

The finding of $f_j(r')$ cannot be carried out by the solution of the
full Eq. [5] with the proper boundary conditions on the particle
$(v(r) = U(r) = {}^t U(r) + \omega \times x$ for $r \longrightarrow s + b)$ and
on the wall $(v(r) = 0)$. Thus, one uses as an approximation for $s \gg b$
(Fig.1) an "outer expansion" in which

$$v_i(r) = \int_{-l}^{l} \tau_j(r') \, u_{ij}(r, r') \, dr' \qquad [8]$$

only, and for $\frac{1}{\tau} \lesssim \varsigma \ll l$ (for which the disturbance can be assumed to evolve from a portion of an <u>infinite straight</u> cylinder of radius $\xi_{r'}$, an "inner expansion" (6)

$$v_{1'}(r) = \frac{1}{2\pi\mu} C_1'(r) \left[\ln \frac{\xi_s}{\varsigma} + K(s)\right] + U_{1'}(s) \qquad [9]$$

and

$$v_{i'}(r) = \frac{1}{4\pi\mu} C'(r) \left[\ln \frac{\xi_s}{\varsigma} + \frac{\varsigma_i \varsigma_j}{\varsigma^2} + K_{ij}(s)\right] + U_{i'} \qquad [10]$$

where $1'$, i' ($= 2$, 3) respectively stand for the particle-locked local coordinates $x_{1'}$, $x_{2'}$, $x_{3'}$, C_1', C_j' are quantities affected by the wall and K, K_{ij} are constants defined by the geometry of the cross-section at e' (Fig. 1). This "inner expansion" can be also written in the vectorial form fit for any coordinate system

$$4\pi\mu \, v(r) = M \cdot C \ln \frac{\xi_s}{\varsigma} + M \cdot \pi \cdot C + I \cdot C - I' \cdot C + 4\pi\mu \, U \qquad [11]$$

where M, C, π, I, I' are defined in APPENDIX 1.

The two approximations are matched in a region in which they are both assumed to hold $(\xi \ll \varsigma \ll l)$, and the relevant constants so derived.

In the case of the "outer expansion", one can write

$$u_{ij}(r, r') = U_{ij}^{\infty}(r, r') + u_{ij}^{w}(r, r') \qquad [12]$$

where $u_{ij}^{\sim}(r, r')$ has singularities on the particles axis

and $u_{ij}^{w}(r, r')$ is non-singular when $\rho \gg \mathcal{b}$.

b. Straight Body

In this case Eq. [8] is integrated by Batchelor's approximation to [11] (6)

which gives

$$4\pi\mu \, \mathbf{v}(r) = \left\{ \frac{1}{\sigma} + \ln\left[\frac{(1 - x^2/\ell^2)^{1/2}}{\lambda} \right] \right\} M \cdot f + M \cdot f \ln \frac{\mathcal{b}_s}{\rho}$$

$$- I''\cdot f + - M \cdot R + \Lambda + I \cdot f \qquad [13]$$

I'', R and Λ being defined in APPENDIX 1 , $\sigma = [\ln(2\ell/\mathcal{b})]^{-1}$

and $\lambda = (\mathcal{b}_{r'}/\mathcal{b})$. Now, matching the coefficients of the

(singular) $\ln \frac{\mathcal{b}_s}{\rho}$ part in [11] and [13] , one gets

$$C(s) = f(s) \quad , \qquad [14]$$

and, doing the same for the non-singular part,

$$4\pi\mu \, U(s) = \left\{ \frac{1}{\sigma} + \ln\left[\frac{(1 - x^2/\ell^2)^{1/2}}{\lambda} \right] \right\} M \cdot f + I^0 - \pi^0 \cdot f + \frac{1}{2} M \cdot R + \Lambda \qquad [15]$$

where $I^0 = -I'' + \frac{1}{2} I'$ and $\pi^0 = \pi \cdot M$.

At this stage $f_i(s)$ can be **numerically calculated** from [15]

by dividing our particles' axis into N equal parts, to each of which is

associated an average $f_i(s)$, and performing the integration of

$u_{ij}^w(r, r')$ and $\frac{1}{|s-r'|}$ respectively appearing in

Λ and R ; so, for the two-dimensional case of particles' motion,

one obtains 2 N equations for 2 N unknowns while for the three-

dimensional case one obtains 3 N equations for 3 N unknowns.

According to Batchelor (6), it is possible to use here a quick iterative

method by writing

$$f_j(s) = \sigma f_j^{(1)}(s) + \sigma^2 f_j^{(2)}(s) + \sigma^3 f_j^{(3)}(s) + \cdots \qquad [16]$$

i.The_Wall_Effect

Dealing with a cylindrical particle undergoing a translational

and rotational motion near a planar solid wall (Fig. 2) and statisfying
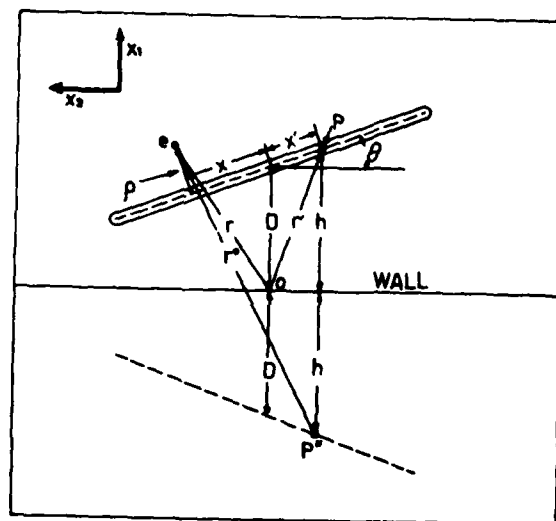
Fig.2. A slender cylinder-planar solid wall system, coordinates
     used in analysis,

the no-slip condition on all boundaries, one has to introduce on the

reflected image of the particles' axis a line-distribution of point

forces, $-f_i(x)$, a line distribution of doublets, $2h f_i(x)$,

and a line distribution of quadrupoles, $-4h^2 f_i(x)$ (8) .

- 12 -

In this case

$$u_{ij}^{\infty}(r, r') = \frac{\delta_{ij}}{|r - r'|} - \frac{(r_i - r_i')(r_j - r_j')}{|r - r'|^3} \qquad [17]$$

and

$$u_{ij}^{W}(r, r') = \frac{\delta_{ij}}{|r^*|} - \frac{(r_i - r_i')(r_j - r_j')}{r^{*3}} + 2h(x)(\delta_{j\alpha}\delta_{\alpha k} - \delta_{j3}\delta_{3k})$$

$$\times \frac{h\delta_{ik}}{|r^*|^3} - \frac{3h r_i^* r_k^*}{|r^*|^5} - \frac{\delta_{ik} r_3^* + \delta_{3k} r_k^*}{|r^*|^3} - \frac{3 r_i^* \cdot r_k^* \cdot r_3^*}{|r^*|^5} \qquad [18]$$

where α is 1 or 2 and i, j, k = 1,2,3 respectively .

ii. Motion within a Flow

Similarly to the "outer expansion" in a quiet medium, it is possible
to write in this case for $6/\varsigma \ll 1$

$$v'(r) = \int_{-l}^{l} f_j(r) u_{ij}(r, r') dr' \qquad [19]$$

In which $v'(r) = v(r) - v^*(r)$ and $v^*(r)$ is the
undisturbed flow $(v(r) \rightarrow v^*(r)$ as $r \rightarrow \infty)$; the
"inner expansion" can be expressed by an equation similar to [11]
but where $C = (C_1', C_2', C_3')$ is now affected by the
flow.

Thus, after performing the necessary matching between [19] and the
modified [11], one gets like [15]

$$4\pi\mu\, U'(s) = \left\{ \frac{1}{\sigma} + \ln\left[\frac{(1-x^2/\rho^2)^{1/2}}{\lambda}\right] \right\} M \cdot f(s) + I^{(0)} \cdot f(s$$

$$- \pi \cdot M \cdot f(s) + \frac{1}{2} M \cdot R + \Lambda(s) \qquad [20]$$

in which $U'(s) = U(s) - v^*(s)$, $U(s)$ is defined by
$v(r) \longrightarrow U(r)$ for $r \longrightarrow \delta + b$, and all other symbols are
as marked above.

Expanding $v^*(r)$ on the (straight) particles' axis in the
form

$$v_i^*(x) = B_i^{(0)} + B_i^{(1)} x + B_i^{(2)} x^2 + \cdots \qquad [21]$$

and putting $x_k = x\, i_k$ (i_1 being $\cos\theta$ and i_2 being $\sin\theta$),
one has for $U'(s)$

$$U_i'(x) = U_i(x) - v_i^*(x) = V_i - B_i x - B_i^{(2)} x^2 - \cdots \qquad [22]$$

where $B_i = \epsilon_{ijk}\,\omega_j\, i_k - B_i^{(1)}$, ω_i is the rotational velocity
of the particle and V_i is its translational velocity.

2. Computational Procedure

The trajections of our particle were derived from the solution of Eqs. [1]
and [2] on the specific assumptions that the particles are:

    i. homogeneously dense

and

    ii. affected only by the gravitational force $m\mathbf{g}$, the fluiddynamic
force $\mathbf{F_F}$ (Eq. [6]) and the fluiddynamic torque $\mathbf{L_F}$.

    At first were treated two-dimensional cases, in which particles axis
stays in a plane containing $\mathbf{g}$; then we considered three dimensional
situations.

For the two-dimensional cases, where the [1] and [2] turn into

$$m\, d\mathbf{V}/dt = (m - m')\mathbf{g} + \mathbf{F_F} \qquad [23]$$

and (since $\omega_1 = \omega_2 = 0$)

$$I_3^* \,\omega_3 = L_3 \,, \qquad [24]$$

we employed:

    i. A quick technique based on Eq. [16]

and

    ii An elaborate technique described in APPENDIX 1.

The computation itself was performed (on the Hebrew University CYBER 74 CDC com-
puter) by the use of a fourth-order Runge-Kutta method; the time intervals
were from $5 \cdot 10^{-4}$ to $3 \cdot 10^{-4}$ second, depending on the (decreasing)
gap between the particle and the wall.

II. Experimental

The experiments were essentially intended to check the calculations in their significant points. Thus, one could in principle either:

1. Determine the force F_F and torque L_F from measured trajectories and orientations and compare with theory

or

2. Determine the whole trajectories of the particles with their orientations and test against computations.

At any case it was necessary to measure particles' location and orientation as a function of time; so, since the observation of small cylindrical aerosol particles is complicated by light scattering phenomena (10), it was thought worthwhile to use large (macro) particles which move in oil in a creeping motion ($Re \ll 1$) too.

1. Method

In essence and without loss of generality, our experiments were carried out by/a two-dimensional motion of a homogeneously dense cylindrical body falling under the action of gravitation in an oil medium. Here, out of the above two alternatives, we chose the latter which is more exact than the former as it does not involve differentiation of location and velocity data curves.

2. Apparatus

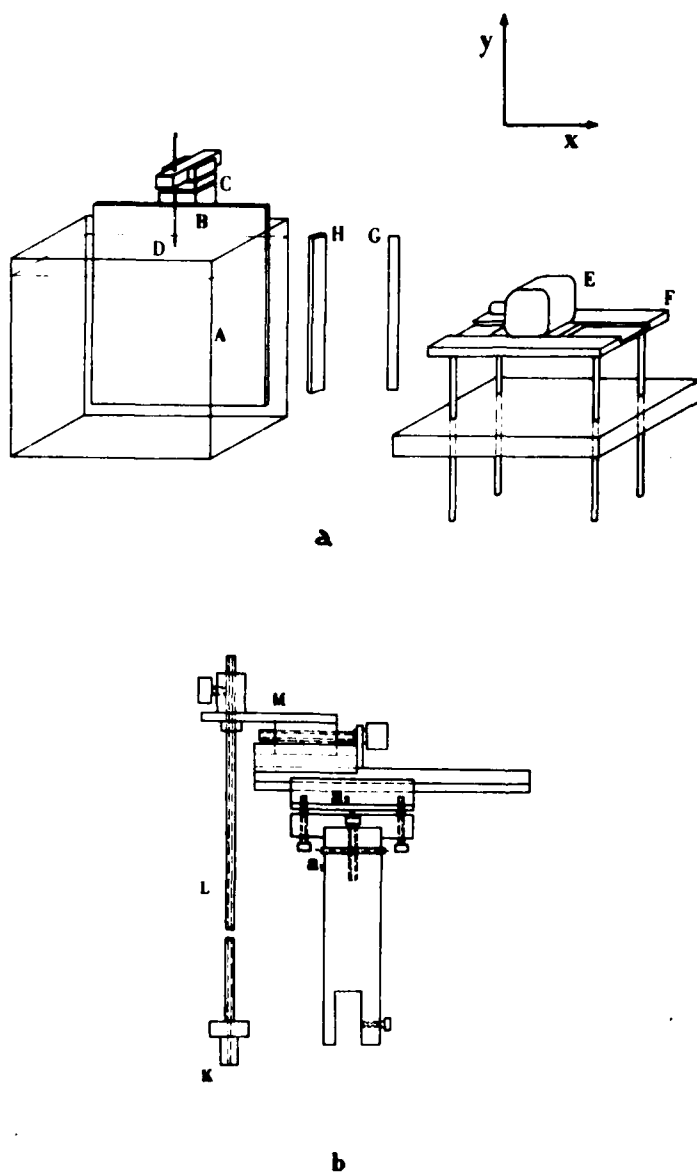The apparatus designed and constructed for the above purpose (Fig. 3,a and b) consisted of:

Fig. 3. The experimental apparatus (achematical) (a) A, Tank;
B, plate (wall);C, release device; D, cylinder; E, movie-camera; F, platform;
G, scale, H, mirror. (b) K, cylinders' holding part of release device;
L,M, sliding rod and guide, respectively, a_1, a_2 pivote rods.

A tank A containing silicone oil in which was suspended a polished steel plate B, a device C to release a metallic cylinder C into the liquid, a movie-camera E and light source for the trajectory photographing, a moving platform F for the camera, and a scale G -mirror - light source combination for locating the particle.

The tank was made of Plexiglas in the (inner) dimensions of 50 cm height, 50 cm. breadth and 3 cm. width and was kept <u>vertical</u> by its own weight. The liquid (F 111/10000 dimethyl silicone fluid, ICI, England) had a (nominal)viscosity μ of 10^4 centistokes or about 100 poise dynamic viscosity at 25°C with a temperature coefficient of 0.02 %./$^\circ$C, and a density of 0.968 g. cm^{-3} at 25°C. This liquid was satisfactorily Newtonian as tested before each experiments by measuring μ at various shear rates $\partial v_i / \partial x_j$ by the settling velocity of various sized Stokesian steel balls. The cylinder used as a tested particle had a radius b of 0.0075 cm, a semi-length l of 1.5 cm. and a density of 7.780 g. cm^{-3}. It was introduced into the liquid by a slow sliding movement in the groove of the devices' edge K (Fig. 3 b) and along the middle (vertical) line of the plate (wall). The camera was a Bolex H 16 Reflex movie instrument (Baillard, Switzerland) equipped with a 1: 18 lens.

3. Procedure

The viscosity μ of the liquid was determined before every run as described above; it was found to be constant, within the experimental error, at the value of 112 $\pm$ 2 poise for 16.4°C. The temperature of the oil, measured at various locations in the tank, was constant to a degree of 0.02°C, which amounted to a viscosity change of 0.02 poise. The trajectory photographing was performed while keeping the center of the falling cylinder on the optical axis of the camera as well as possible. The reading of position and orientation of the particles image on the movie film was carried out with a Nikon 6CT2 profile projector (Nikon, Japan) to a (nominal) accuracy of $\pm$ 0.001 mm.

Here it should be pointed out about the critical requirement of two-dimensionality to which a self-restriction was imposed. Due to the cylindrical rod release-operation, there was always a chance that the particle will not move with its axis in the plane of g . So, in every experiment, the film image of the falling rod was aposteriori checked against the expected value deduced from the actual size and orientation of the body, and, when a deviation occured, this run was discarded.

III. Results

As the checking experiments had to be restricted to a liquid medium and macro particles, the calculations were confined to that situation too. Dealing with physical cases which can be analyzed by continuous, classical fluiddynamic methods, this did not matter as long as creeping motion conditions ($Re \ll 1$, $Kn \ll 1$) still prevailed and the liquid specific effects associated with the acceleration of the particles, viz. the

added mass and moments of inertia and the Basset term influence (11),
could be neglected.

The cases selected for computation were chosen to be a two-dimensional
motion in a still environment near:

    i. A vertical wall (Figs. 5 through 8),

    ii. An horizontal wall (Figs. 9 through 11),

    iii. An inclined wall (Figs. 12 through 19)

and a two-dimensional motion within:

    i. A two-dimensional Couette flow over an horizontal wall (Fig. 20)

    ii. A two-dimensional Poiseuille flow through an horizontal channel
       (Fig. 21).

All of these cases simulate real situations. Thus, for example, if the
particles are small enough, then any corrugated surface can be represented
by inter-connected plan ar portions of various inclinations to the horizontal;
likewise, a general laminar field can be approximated by a series of inter-
adjoining Couette flows. The restriction to two-dimensional motion which
is relaxed latter on in a further study (not reported here) is not serious
since in many instances such a situation is indicative enough of the physical
occurences.

The distances and angles employed in the calculations are brought out
in Fig. 4 (the unit of distance is always the semi-length 1). Thus the
undisturbed Couette flow was expressed by

$$V_2^{*}(x_1) = k_1 D_1 \qquad\qquad [25]$$

where κ is the (constant) velocity gradient, while the (undisturbed) Poiseuille flow was given by

$$V_2^* (x_1) = k_2 (a^2 - D_1^2) \qquad [26]$$

where k_2 is a (flow) constant and a is the half width of the channel. The typical results shown here are presented in terms of the (operationally) *important* drift displacements and linear velocities and the intuition-assisting rotational velocities and particle orientation.
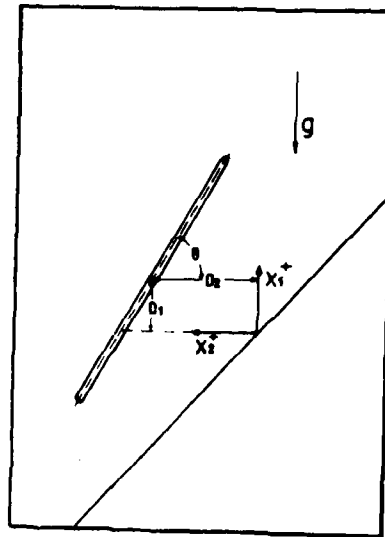

Fig. 4. A slender body near a wall. Distances
and angles used in calculations.
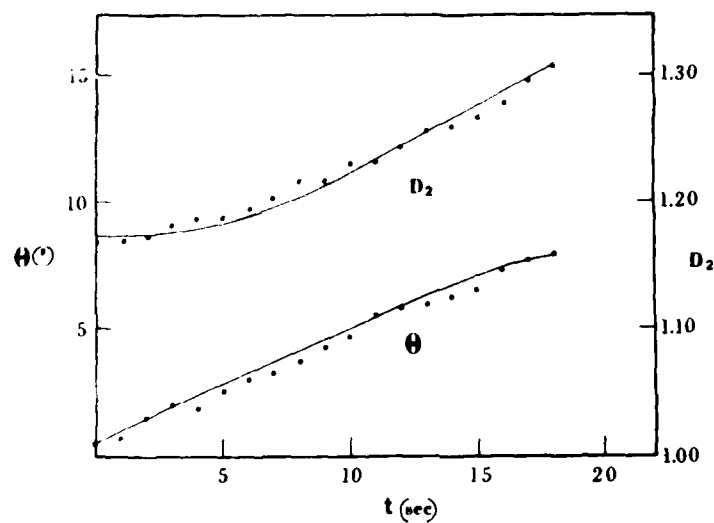
A Quiet Medium

Fig. 5. Drift displacement and orientation of a cylinder
near a vertical wall as a function of time.

$D_{2,c} = 1.168\, l$, $\theta_o = 1^\circ$ ($\theta = \pi/2 - \theta$) ; $l = 1.5$ cm;
$b = 0.075$ cm. ; $\rho_p = 7.780$ g. cm^{-3}; $\mu = 100$ poise;
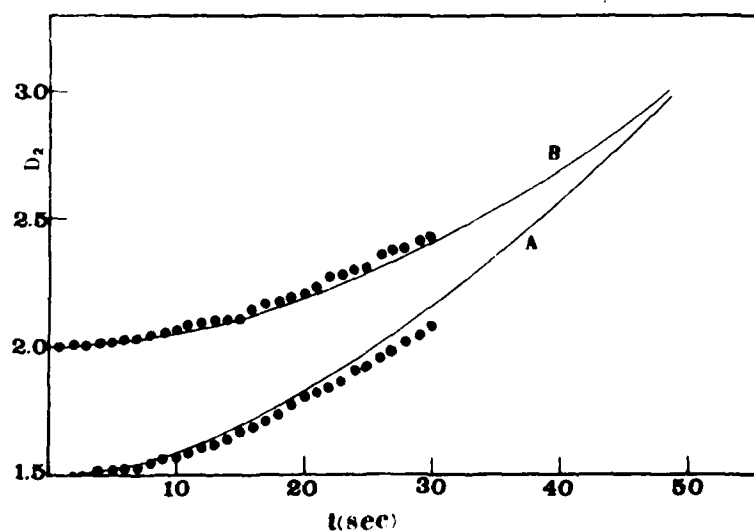•,experimental; —,theoretical

Fig. 6. Drift displacement and orientation of a cylinder near a
vertical wall as a function of time. Same parameters as
of Fig. 5 except for : A. $D_{2,c} = 1.5\, l$; $\theta_o = 89^\circ$. B: $\theta_o = 21$,
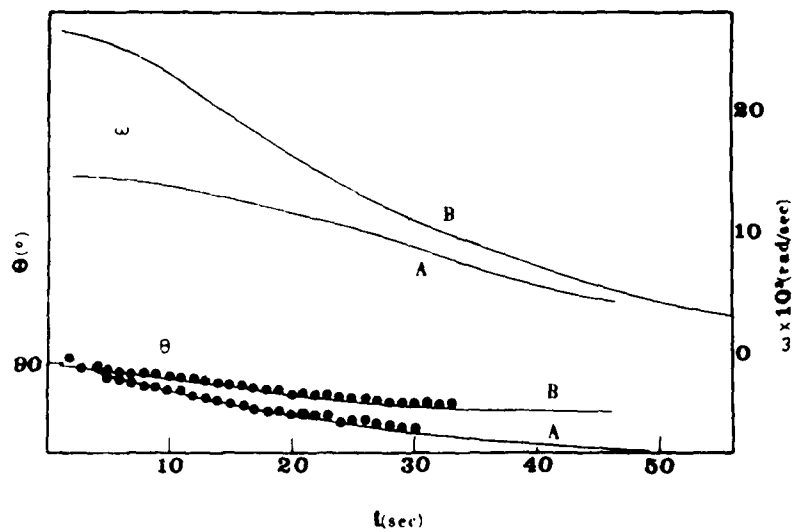$\theta_o = 93^\circ$.

Fig. 7. Orientation and angular velocity of a cylinder near
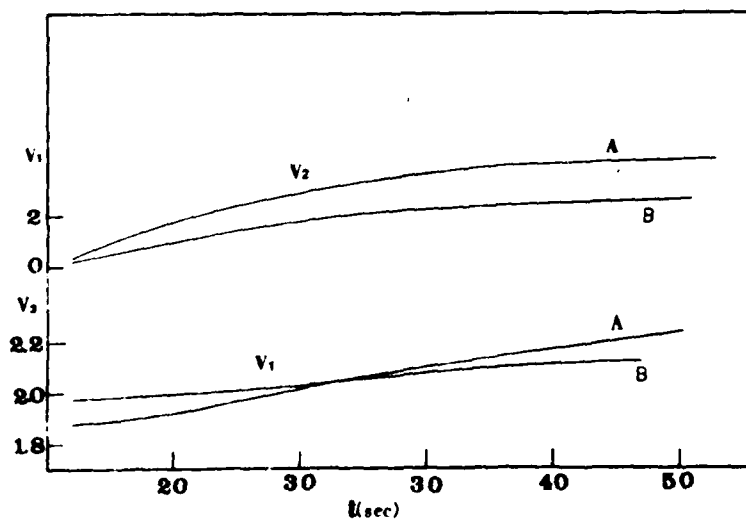a vertical wall as a function of time, for cases
A,B of Fig. 6.

Fig. 8. Vertical (V_1) and horizontal (V_2) velocities (in 1/sec)
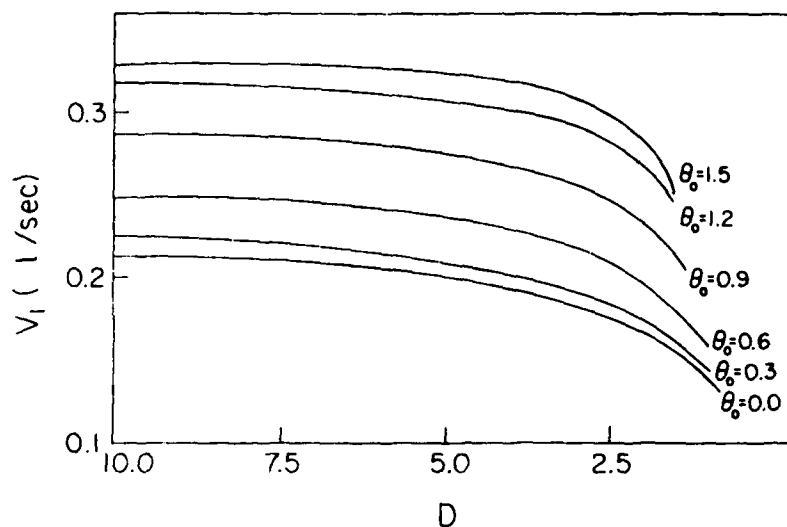of a cylinder near a vertical wall for cases A and B of
Fig. 6.

Fig. 9. Vertical velocity of a cylinder falling towards
an horizontal plane as a function of D_1 and for
various initial orientations Θ_o (in rads).
Same cylinder's and liquid's properties as of Fig.5.
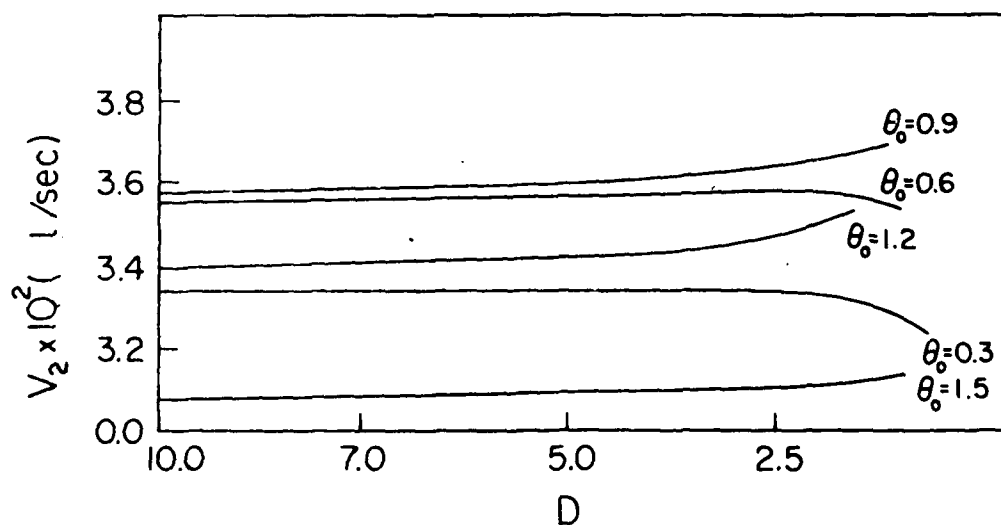$D_{1,o} = 10 \, l$.

Fig. 10. Drift (horizontal) velocity of a cylinder falling towards
an horizontal plane for various initial orientations Θ_o
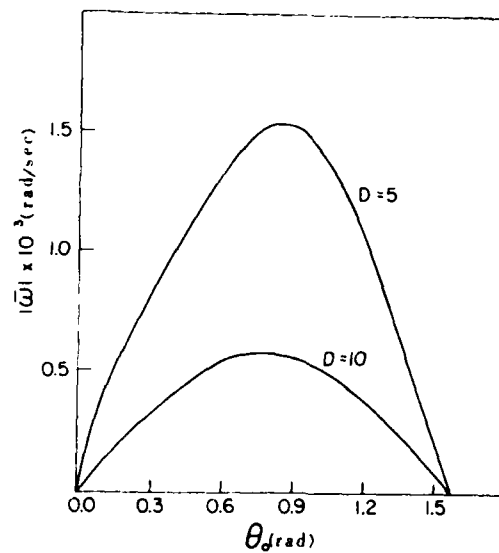(in rads). Same cylinder's and liquid's properties as of Fig.5.
$D_{1,o} = 10 \, 1$.

Fig. 11. Angular velocity of a cylinder falling towards an horizontal
plane for various initial orientations (in rads) at $\mathcal{D}_{1,c}$

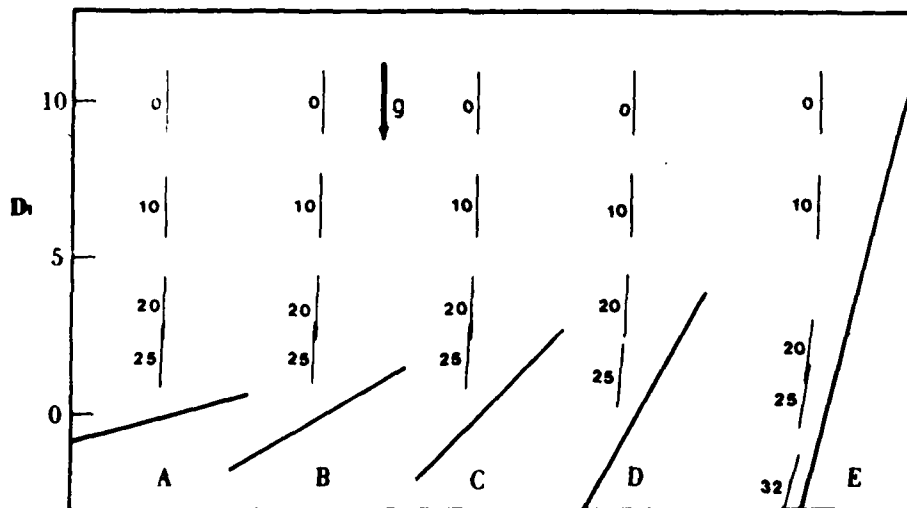= 10 1, 5 1. Same cylinders' and liquids properties as of Fig.5.

Fig. 12. Time history of a cylinder falling towards a plane inclined to
the horizontal at angles: A-15°, B-30°, C-45°, D-60°,E-75°;
initial orientation - vertical; $\mathcal{D}_{1,o}$ = 10 1. Numbers near
positions indicate elapsed time in seconds. Same cylinder's and
medium's properties as of Fig. 5.
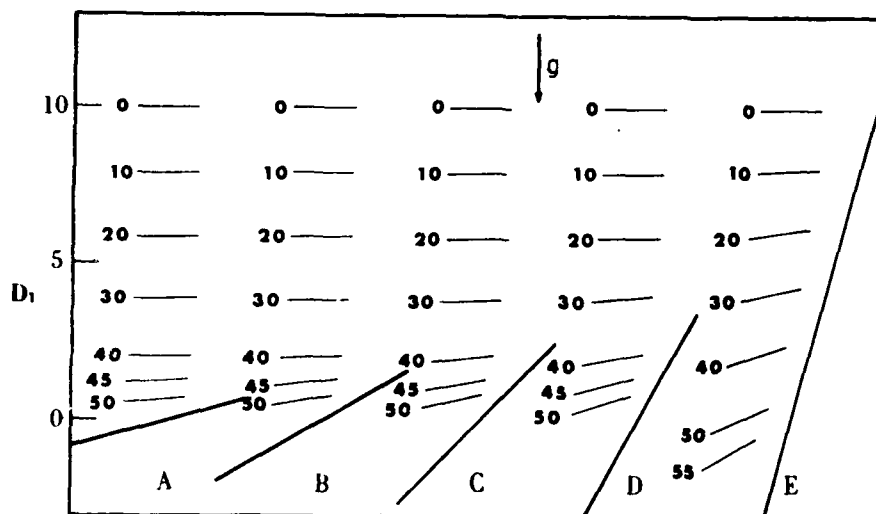
Fig. 13. Time history of a cylinder falling towards an inclined plane.
Same parameters as of Fig. 12 except for horizontal initial
orientation.
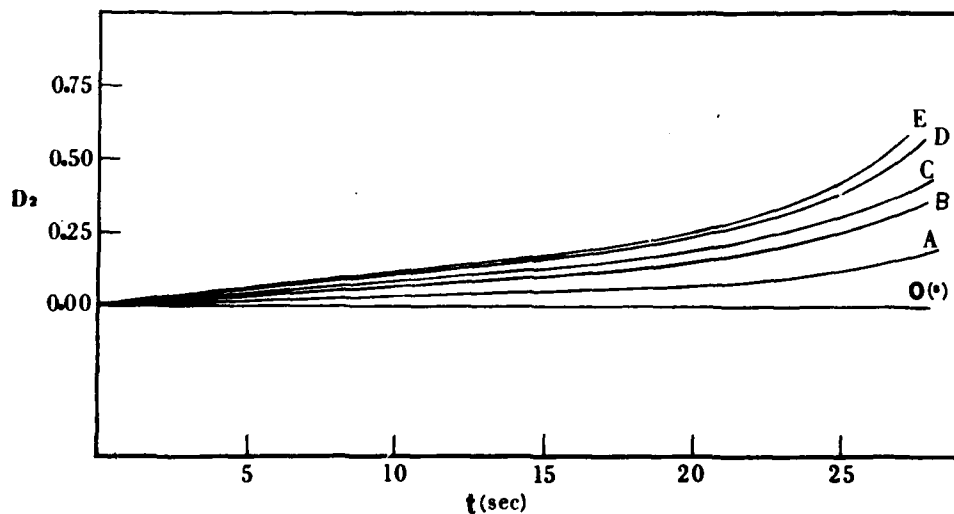
Fig. 14. Drift displacement of a cylinder falling towards an inclined
plane. Same parameters and conditions as of Fig. 12.

Fig. 15. Drift displacement of a cylinder falling towards an inclined
plane. Same parameters and conditions as of Fig. 13.
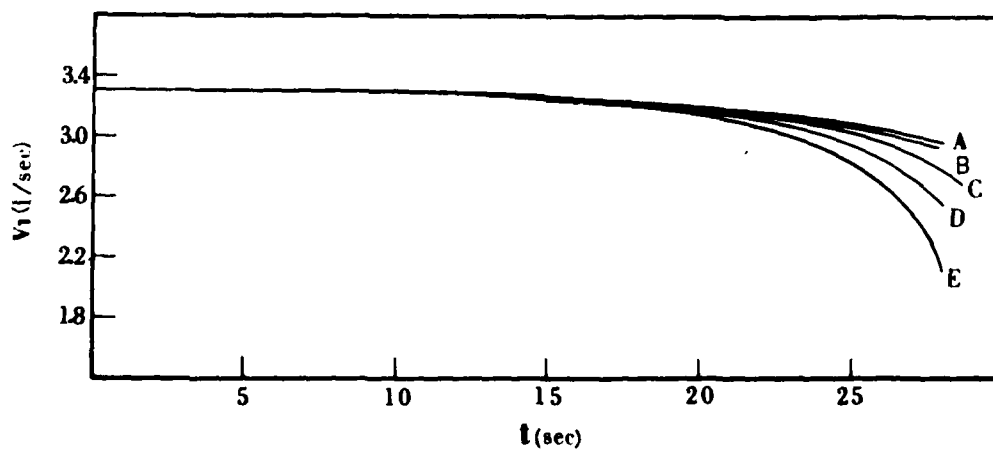
Fig. 16. Vertical velocity of a cylinder falling towards an inclined
plane. Same parameters and conditions as of Fig. 12.
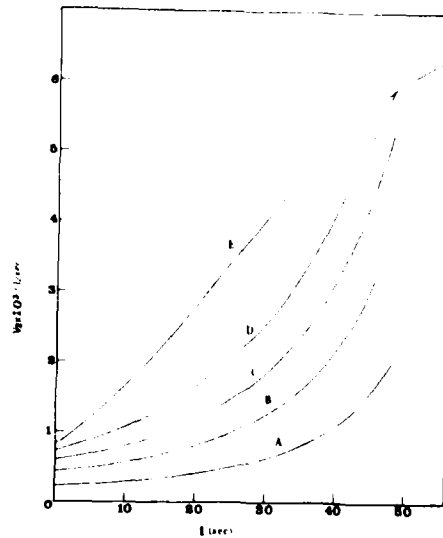
Fig. 17. Drift (horizontal) velocity of a cylinder falling towards an inclined plane. Same parameters and conditions as of Fig.13.
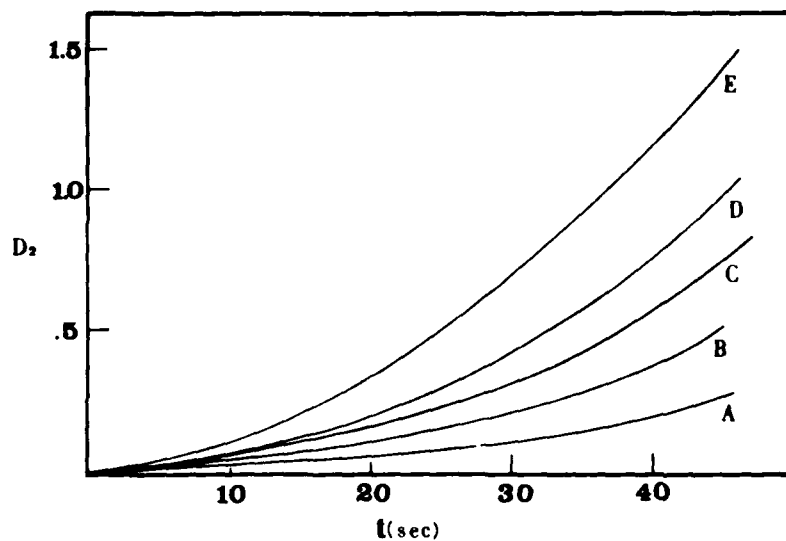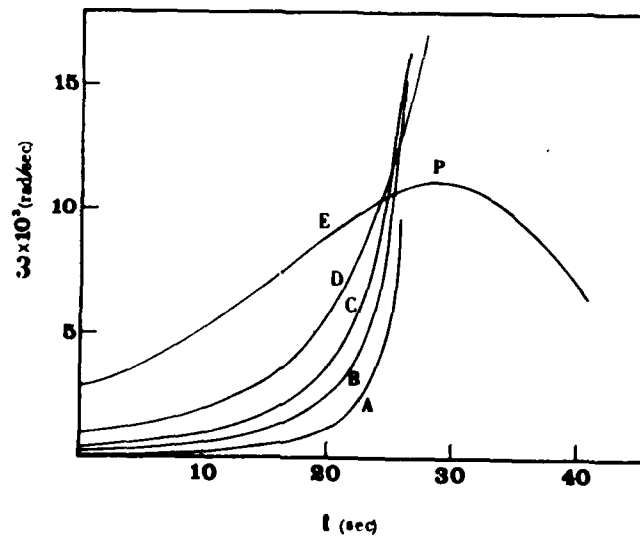

Fig. 18. Angular velocity of a cylinder falling towards an inclined plane. Same parameters and conditions as of Fig. 12. $(D_2$ reaches a minimum at the point P).
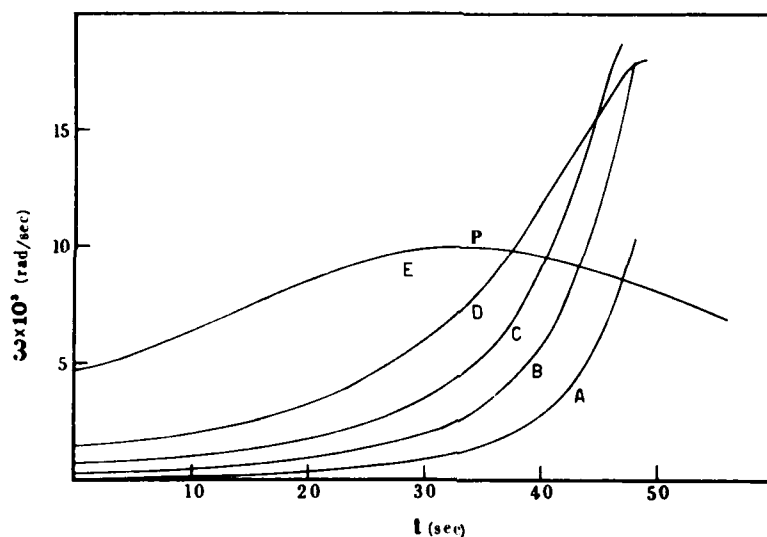
Fig. 19. Angular velocity of a cylinder falling towards an inclined
plane. Same parameters and conditions as of Fig. 13. (D_2
reaches a minimum at the point P.).

Motion within a Flow
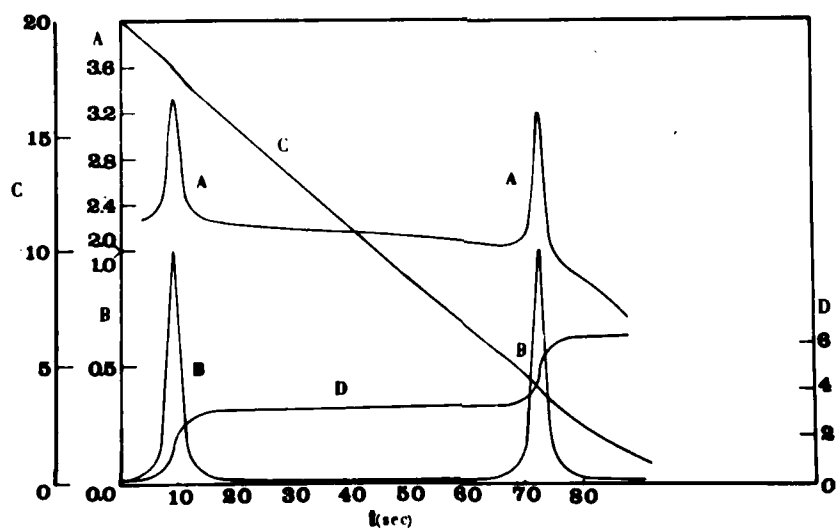
Fig. 20. Change with time of the vertical velocity, A (in 1/sec),angular
velocity B (in rads/sec), distance from the wall C (in 1) , and
orientation angle D(in rads) of a cylinder within a Couette flow.
$D_{1,2}$ =20 1.
Same cylinders and liquids properties as of Fig. 5.
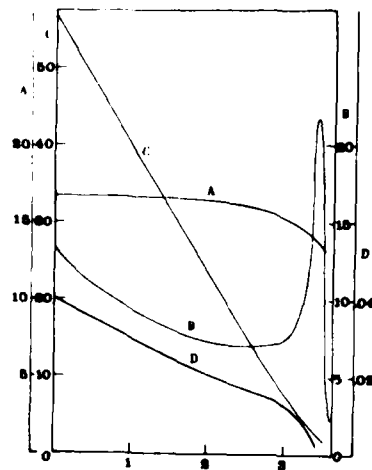
Fig. 21. The vertical velocity A (in 1/sec), angular velocity B
(in rads/sec), distance from the wall C (inl), and orientation
angle D (in rads) as a function of time. Medium-air of μ
$= 1.718 \times 10^{-4}$ poise; particle - 1 = 20 μm ; b = 0.5 μm;
ς_p =2.23 g. cm^{-3}; channels half width a = 0.5 cm;
$k_\perp = 0.15 \ (1 \cdot sec)^{-1}$.

IV. Discussion

The results shown in the above figures should be discussed while keeping in mind the behaviour of a cylinder under creeping motion conditions in an unbounded (far from walls) fluid. In the latter case, an homogeneously dense cylinder which settles down in an external field devoid of orienting forces moves with a neutral stability, viz. a fixed orientation angle (12). In our case, however, the cylinder is definitely subjected to a torque.

Vertical Wall; Still Medium

Here one can observe:

i. A continuous change of the orientation angle θ caused by the wall-created torque,

ii. A continuous development of a drift and an increase of the displacement D_2.

It turns out that the sign of the torque depends on the angle θ ;for every initial distance of the particle from the wall there exists a critical angle θ^* such that

$$L_F < 0 \qquad \text{when} \quad |\theta| > \theta^* ,$$

$$L_F > 0 \qquad \text{when} \quad |\theta| < \theta^* ,$$

and

$$L_F = 0 \qquad \text{when} \quad |\theta| = \theta^* .$$

The correspondence between theory and experiments depicted in Figs. 5 through 7 is really good, which produces a confidence in our calculational method.

Horizontal Wall; Still Medium

Here particles motion is always two-dimensional. Its characteristics are·

    i. A continuous decrease of the sedimentation velocity, V_1, as the plane is approached,

    ii. An enhanced wall influence for small θ_0 ,

    iii. A negligigble effect for large $\theta_0 (> 0.3)$;

    iv. An increased value and sensitivity to θ_0 of the angular velocity as the particle-plane gap is reduced,

    v. A constant drift velocity, V_2 , till very small distances from the plane.

It is interesting to compare these results with those of a spherical particle-horizontal wall situation(2) where a similar behaviour is observed.

Inclined Wall; Still Medium; Two-dimensional Situation

From the results for the inclined wall it is seen that:

    i. In the case of a vertical initial orientation, the torque is positive, which will cause the cylinder to drift from right to the left (Fig.12).

    ii. In the case of an horizontal initial orientation, the torque is negative but, nevertheless,the cylinder will drift in the former direction too (Fig. 13).

    iii. In the case of a wall-inclination of a little less than 75° for a vertical initial cylinder-orientation and of a little less than 60° for an horizontal wall-inclination, the angular velocity ω and the horizontal separation D_2 respectively reach a minimum and a maximum at the same time. Thus, the particle will not collide with the surface, which is of a great significance.

Here one should note the aerosol specificity as compared to the motion within our liquid. Since both the mass and the moment of inertia of a cylindrical particle are proportional to b^2, it comes out that the thinner is the particle the greater are its translational (in l/sec) and rotational velocities attained after a certain time. However, if one returns to dimensional quantities, one observes that the overall particle drifts in aerosol and liquid systems, as caused by a plan ar wall, will still be the same. For an aerosol system, the influence of the wall is manifested already at distances of about 50 l (2).

Motion within a Flow; Two-dimensional Situation

Couette Flow

From Fig. 20 it can be seen that the behaviour of our cylinder as it rotates in the gradient flow is essentially the same as that far from a wall ("Deposition from Flow", Final Report DAERO-76-G-14, 1978, and Gallily and Eisner, J. Colloid Interface Sci. 68, 320-37 (1979)). The wall effect is shown in the decrease of the second maximum of the vertical velocity V_t as the particle nears the horizontal plane (curve A); the effect is, however, over-shadowed in the angular velocity B curve. It is noteworthy that the (rotating) particle spends more than 85% of its time in an horizontal orientation.

Poiseuille Flow

The behaviour in this case is essentially the same as that within a Couette flow.

General Conclusions

i. For cylindrical particles there is a pronounced wall effect which may be of a great importance in a motion within small cavities like those of the human lung, and near small aerosol collecting obstacles.

ii. The sedimentation efficiency of the particles on an inclined or horizontal plane is decreased due to the effect.

iii. The surface concentration of the particles' deposit on an inclined plane has a greater dispersion as compared to that for which the wall does not exert any influence.

iv. The collision of the particles with a vertical wall is very small due to their "repulsion" from it; only particles with $0 < \theta < \pi/2$ will have a slight chance of colliding.

Finally, extending the results to motion near curved convex surfaces, one can assume that the smaller is the angle between the tangent plane and the surface, the greater is the (still medium) collision efficiency which is defined as the ratio between the number of settled particles to the number that would have sedimented had all trajectories been vertical.

V. Applications

The slender body method of calculating the fluiddynamic force and torque on the particles seems to be more useful than that based on Oberbeck's (4) and Jeffery's (5) equations since it does not depend on any limiting assumptions concerning the flow in which the particle is immersed. For example, any numerically (computer) solved field of flow can be introduced into the slender body equations where it is necessary to know the undisturbed velocity

(Eq. 19) at the middle of each of the N divided cylinder's sections.

This has been performed (with no wall effect,however) in a DFG (Germany) supported study in calculations which checked quite satisfactorily with experiments (13).

B. BROWNIAN DIFFUSION

I. Theoretical

  1. Method

a. General

The diffusion of aerosol particles in air is generally controlled by a Brownian, a turbulent or a mixed mechanism; near surfaces, where turbulence subsides, it is dictated mainly by the first.

In the case of spherical particles, there has been already much study on the numerous aspects of Brownian diffusion, but, very little has been performed with regard to the process for the nonspherical counterparts. The difficulty arises from the general non-isotropic nature of teh fluiddynamic interaction between particles and medium which makes it necessary to consider the spatial orientation and the rotation of the former.

A useful way of treating the problem is based on Brenner's formal structure (14) in which one assumes a six-dimensional location-orientation hyperspace where the general number concentration is given by the solution of the conser-vation -equation

$$\frac{\partial \sigma}{\partial t} + \frac{\partial}{\partial r} \cdot \overset{t}{\mathbf{J}} + \frac{\partial}{\partial \phi} \cdot \overset{r}{\mathbf{J}} = 0 \qquad [27]$$

Here, the translational, $\overset{t}{\mathbf{J}}$, and rotational, $\overset{r}{\mathbf{J}}$, fluxes are respectively expressed (for axi-symmetrical particles, for example) by

$$\left. \begin{array}{l} \overset{t}{\mathbf{J}} = -\overset{t}{\mathbf{D}} \cdot \dfrac{\partial \ln \sigma}{\partial r} + \sigma u \\[20pt] \\ \overset{r}{\mathbf{J}} = -\overset{r}{\mathbf{D}} \dfrac{\partial \sigma}{\partial e} + \sigma \dot{e} \end{array} \right\} \qquad [28]$$

and

For the physical applications of diffusion, where one needs to have ensemble orientation-averaged quantities, it is useful to define a total concentration c, translational flux $\overset{t}{\mathbf{J}}_\mathsf{T}$, averaged translational velocity $\langle u \rangle$ and a diffusion diadic $\overset{t}{\mathbf{D}}_\mathsf{T}$ by

$$\begin{pmatrix} c \\[6pt] \overset{t}{\mathbf{J}}_\mathsf{T} \\[6pt] \langle u \rangle \\[6pt] \overset{t}{\mathbf{D}}_\mathsf{T} \end{pmatrix} = \begin{pmatrix} \displaystyle\int_\phi \sigma \, d^3\phi \\[10pt] \displaystyle\int_\phi \overset{t}{\mathbf{J}} \, d^3\phi \\[10pt] \dfrac{1}{c} \displaystyle\int_\phi \sigma u \, d^3\phi \\[10pt] \dfrac{1}{c} \displaystyle\int_\phi \overset{t}{\mathbf{D}} \sigma \, d^3\phi \end{pmatrix} \qquad [29]$$

The total, orientation-averaged translational diffusion diadic $\overset{t}{\mathbf{D}}_\mathsf{T}$ is the operational parameter to be plugged into the (translational) diffusion equation of the aerosol ensemble. It is dependent on the orientation distribution function of the particles which is the most important property of the ensemble.

In Brenners' (formal) treatment (14) and for an axi-symmetric particles' case, one has instead of [27]

$$\frac{\partial \sigma}{\partial t} + \frac{\partial}{\partial r} \cdot \overset{\leftrightarrow}{J} + \frac{\partial}{\partial e} \cdot \overset{\rightharpoonup}{j}' = 0 \qquad\qquad [30]$$

where $\quad \overset{\rightharpoonup}{j} = - \overset{\leftrightarrow}{D}_{\perp} \frac{\partial \sigma}{\partial e} + \sigma u \quad$,and

$$\sigma(r, e, t) = c(r, t) f(r, e, t) \quad . \qquad [31]$$

In that case, one obtains for the orientation distribution density f the governing equation

$$\partial f / \partial t + \frac{\partial}{\partial e} \cdot \overset{\rightharpoonup}{j}' = X(r, e, t) \qquad\qquad [32]$$

which takes, for example, the form

$$\frac{\partial \sigma}{\partial t} + \overset{r}{P_e} \frac{\partial \sigma}{\partial \phi} = \frac{1}{\sin\theta} \frac{\partial}{\partial \theta}\left(\sin\theta \frac{\partial \sigma}{\partial \theta}\right) + \frac{1}{\sin^2\theta} \frac{\partial^2 \sigma}{\partial \phi^2} \qquad [33]$$

where θ, ϕ are the polar angles and the rotational Peclèt number $\overset{r}{P_e}$ is defined by

$$\overset{r}{P_e} \simeq \frac{|\overset{\rightharpoonup}{\xi}|}{\overset{r}{D}_{\perp}} \qquad . \qquad [34]$$

For a **quiet** medium, the orientation density f has been calculated to be

$$f = \left\{ \sum_n \frac{2n+1}{4\pi} P_n^0 (\cos\theta) \exp\left[-n(n+1)\overset{r}{D}_\perp t\right] \right\} \cdot \int_0^\pi f_0\, P_n^0 (\cos\theta_0) \sin\theta_0\, d\theta_0$$

$$+ \sum_{0 < m \le n} \frac{(n-m)!}{(n+m)!} \frac{(2n+1)}{2\pi} P_n^m (\cos\theta)\, \cos m\phi \cdot \exp\left[-n(n+1)\overset{r}{D}_\perp t\right]$$

$$\times \int_0^\pi f_0\, P_n^m (\cos\theta_0)\, \sin\theta_0\, d\theta_0 \quad . \tag{35}$$

For a _flowing_ medium, the convective-rotation equation of axisymmetric

particles for example, viz.

$$\frac{\partial f}{\partial t} = \overset{r}{D}_\perp\, \Delta_r f - \nabla_r \cdot (f\,\omega) \tag{36}$$

has been (firstly) solved by Peterlin (16) when the Couette conditions and the

pertinent Jeffery equations for ω (5) hold. The solution shows f to be a sole

function of the _particle_ Peclet number .

b. The Aerosol Specificity

From the above it can be observed that the (crucial) density function f

for axi-symmetric particles depends on $\overset{r}{D}_\perp$ and ω . The latter have been

calculated in the case of a _liquid_ suspension by classical fluiddynamic

methods (17,5); however, in the case of _aerosol_ systems this is not adequate.

The reason for the inadequacy stems out of the fact that in the very instance

of the only (small) aerosol particles which show a pronounced Brownian motion,

the medium cannot be considered as continuous any more. Thus, both the rotational

diffusion coefficient $^r D_\perp$ and the gradient-rotational velocity of the particles have to be calculated from first principles by statistical-mechanics means.

c. Immediate Aim

It was intended to study (for the first time) the rotational diffusion coefficient of cylindrical or discoidal aerosol particles which form a good geometrical model for many systems. The task has been accomplished, as reported now and also published under the title "On the Stochastic Nature of the Motion of Nonspherical Aerosol Particles III. The Rotational Diffusion Diadic and Applications" by Alfred D. Eisner and Isaiah Gallily, J. Colloid Interface Sci. 81, 214-33 (1981).

The gradient rotational velocity of the particles in a simple (though not limiting) shear flow has been calculated too and presented in the publication:

"On the Stochastic Motion of Nonspherical Aerosol Particles. IV. Gradient Convective Rotational Velocities in a Simple Shear Flow" by Alfred D. Eisner and Isaiah Gallily, J. Colloid Interface Sci. 1982 (in press), which is not included here.

Finally, a third (summarizing) article is in preparation.

d. Medium, Particle, and General Governing Equations

Out of the generalized Einstein equation

$$^\alpha M = {}^\alpha D / kT \quad (\alpha = t, r, c) \tag{37}$$

between the translational, rotational or coupling particle mobility and the
respective diffusion tensors, and from the relation to the operating
torque L_F exemplified by

$$L_F = -\overset{\frown}{M} \cdot \omega \quad ,\qquad\qquad [38]$$

one notes that the core of the calculations is imbedded in the evaluation of
L_F .

The (considered) particles, assumed to be much smaller than the mean free path
$\bar{l}$ of the gas molecules $(\; K_n \;\gg\; 1\;)$,are taken to translate
with a linear uniform velocity U_n with respect to an inertial system
of coordinates O_2 (Fig. 22), and rotate with a uniform velocity ω with
respect to the center of mass M in a quiet medium devoid of external torques.
Thus, the source of L_F is supposed to be only the stochastic bombardment
of the gas molecules.
For our medium (and structureless molecules), the distribution of the molecu-
lar velocities is Maxwellian, i.e.

$$N_{v_2}\, d v_2^{(1)} d v_2^{(2)} d v_2^{(3)} = N\,(h/\pi)^{3/2}\, exp\left[-h\left(v_2^{(1)^2} + v_2^{(2)^2} + v_2^{(3)^2}\right)\right] d v_2^{(1)} d v_2^{(2)} d v_2^{(3)} \quad [39]$$

where (1),(2),(3) respectively stand for x_2, y_2, z_2 and $h = m/2kT$.
Concerning the inertial system O_2 itself, there is no preferred position of
its placement in space since the latter is assumed (by the above) to be
isotropic.
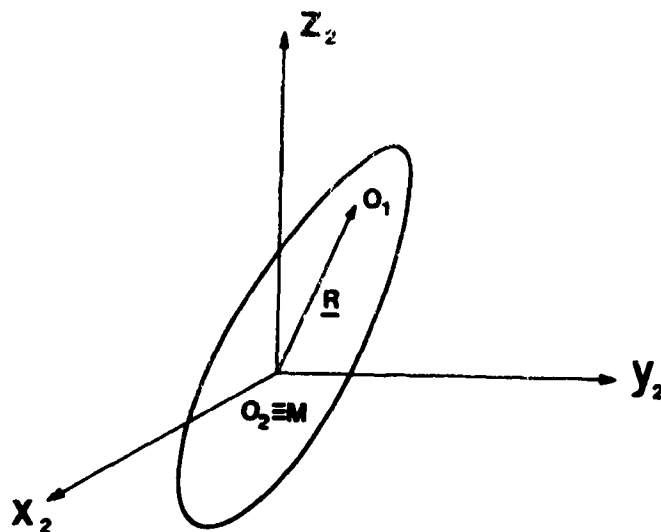
Fig. 22. The external system of
coordinates O_2.

The particles' surface conditions adopted in our analysis are those
of Maxwell (18) according to whom one has to distinguish between a diffusely
reflected fraction α of gas molecules with a Maxwellian distribution
conforming to the surface temperature T_s and a specularly reflected
fraction ($1-\alpha$) for which

$$v_2' = v_2 - 2\,n \cdot (n \cdot v_2) \quad . \tag{40}$$

From the point of view of an observer at 0_2, the velocity of a gas molecule relative to the body-point 0_1 (Fig. 22) is

$$v_1 = v_2 - \omega \times R - U_M \quad . \qquad [41]$$

Thus, the number of these molecules of velocity between v_2 to $v_2 + dv_2$ hitting an elemental surface dS around that point in a unit of time is

$$n^{(in)} d^3v_2 \, dS = -N(h/\pi)^{3/2}[(v_2 - \omega \times R - U_M) \cdot n]$$

$$\cdot \exp[-h|v_2|^2] \, d^3v_2 \, dS \quad , \qquad [42]$$

the momentum transfer at that time is

$$m(v_2 - \omega \times R - U_M) n^{(in)} d^3v_2 \, dS \, , \qquad [43]$$

and the torque imparted to the particles in the k direction is

$$(L_F \cdot k)^{(in)} = -Nm(h/\pi)^{3/2} \iint_{S\ v_2} [k \cdot (R \times (v_2 - \omega \times R - U_M))]$$

$$\times [(v_2 - \omega \times R - U_M) \cdot n] e^{-h|v_2|^2} d^3v_2 \, dS \qquad [44]$$

which is a typical governing equation.

The contribution of the reflected molecules is expressed in a similar fashion but with the exchange of h and N of the velocity distribution of the incoming molecules with h_{τ} and $N^{(r)}$ of the **diffusely** reflected ones as determined by the requirement that (for a steady situation):

    i. The net flux of molecules at each particles surface element is zero;

    ii. The net total **energy** transport at that element is zero, too.

The **total** torque imparted to the rotating-translating particle can be put as

$$(L_F \cdot k)^{(tot)} = (1-\alpha)\left[(L_F \cdot k)^{(in)} + (L_F \cdot k)^{(r)(s)}\right]$$

$$+ \alpha\left[(L_F \cdot k)^{(in)} + (L_F \cdot k)^{(r)(d)}\right] \quad . \qquad [45]$$

2. Calculational Procedure

a. A Spherical Particle

This has been chosen as a test case for the proposed method. Taking here the "natural" coordinates system t_r, t_θ and t_ϕ (Fig. 23), one has

$$R = r(\sin\theta \cos\phi \, i + \sin\theta \sin\phi \, j + \cos\theta \, k), \qquad [46]$$

$$n = \sin\theta \cos\phi \, i + \sin\theta \sin\phi \, j + \cos\theta \, k \quad , \qquad [47]$$

and

$$\begin{pmatrix} v_2^{(1)} \\ v_2^{(2)} \\ v_2^{(3)} \end{pmatrix} = A \begin{pmatrix} v_2^{r} \\ v_2^{\theta} \\ v_2^{\phi} \end{pmatrix} \qquad [48]$$

where A, the transformation matrix is

$$
A = \begin{pmatrix}
\sin\theta\cos\phi & \sin\theta\sin\phi & \cos\theta \\
\cos\theta\cos\phi & \cos\theta\sin\phi & -\sin\theta \\
-\sin\phi & \cos\phi & 0
\end{pmatrix}
\qquad [49]
$$

Fig. 23. The spherical coordinate system.
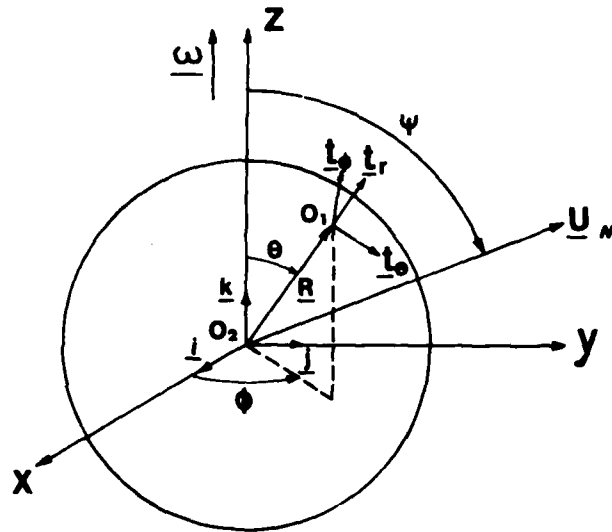
Due to the space isotropy, it is possible to write

$$
\underline{\omega} = \omega\,\underline{k} \qquad\qquad [50]
$$

and

$$
\underline{U}_M = U_M\left(\sin\Psi\,\underline{j} + \cos\Psi\,\underline{k}\right) \qquad\qquad [51]
$$

A sample procedural way for calculating $\left(L_F \cdot k \right)^{(in)}$ for $\Psi = 0$ is given here as follows:

i. The integrand

$$I_1 = k \cdot \left[R \times \left(V_2 - \omega \times R - U_M \right) \right] \left[\left(V_2 - \omega \times R - U_M \right) \cdot n \right]$$

$$= r \sin\theta \, v_2^\theta \, v_2^\phi - r \, U_M \sin\theta \cos\theta \, v_2^\phi - r^2 \omega \sin^2\theta \, v_2^r$$

$$+ r^2 \omega \, U_M \cos\theta \sin^2\theta \quad . \tag{52}$$

ii. Integration boundaries

$$-\infty \leq v_1 \cdot n \leq 0 \quad \text{and so, as} \quad n = t^r$$

$$v_1 \cdot n = v_1^r = v_2^r - U_M \cos\theta \tag{53}$$

which gives

$$-\infty \leq v_2^r \leq U_M \cos\theta \quad . \tag{54}$$

Also, $\quad -\infty \leq v_2^\theta, v_2^\phi \leq \infty \quad . \tag{55}$

iii. Final equation

$$\left(L_F \cdot k \right)^{(in)} = - Nm \left(h/\pi \right)^{3/2} \int_0^{2\pi} \int_0^\pi \int_{-\infty}^\infty \int_{-\infty}^\infty \int_{-\infty}^{U_M \cos\theta} I_1 \cdot$$

$$\times e^{-h \left(v_2^{r^2} + v_2^{\theta^2} + v_2^{\phi^2} \right)} |J| \, d v_2^r \, d v_2^\phi \, d v_2^\theta \, r^2 \sin\theta \, d\phi \tag{56}$$

where $|T$,the velocity components transformation Jacobian is 1.

b. A Cylindrical or Discoidal Particle

Now, the "natural" system of coordinates is t_ρ, t_ϕ and t_z (fig.24).
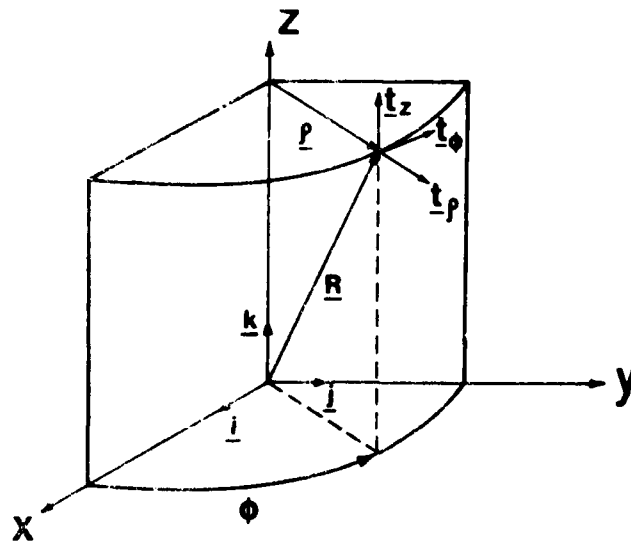
Fig. 24. The cylindrical system of coordinates.

Thus

$$R = \rho \cos\phi\, i + \rho \sin\phi\, j + z\, k \quad , \tag{57}$$

$$t_\rho = \cos\phi\, i + \sin\phi\, j \quad , \tag{58}$$

$$t_\phi = -\sin\phi\, i + \cos\phi\, j \quad ; \tag{59}$$

$$t_z = k \quad , \tag{60}$$

and

$$
\begin{pmatrix} v_2^{(1)} \\ v_2^{(2)} \\ v_2^{(3)} \end{pmatrix} = B \begin{pmatrix} v_2^{\,\xi} \\ v_2^{\,\phi} \\ v_2^{\,z} \end{pmatrix} \qquad [61]
$$

where B, the transformation matrix, is

$$
B = \begin{pmatrix} \cos\phi & \sin\phi & 0 \\ -\sin\phi & \cos\phi & 0 \\ 0 & 0 & 1 \end{pmatrix} . \qquad [62]
$$

Placing the O_2(external) coordinate system (Fig. 24) so that the polar axis of the particle will coincide with k , and assuming an arbitrarily directed angular velocity $\omega = \omega_1 i + \omega_2 j + \omega_3 k$, one can carry out a piecewise calculation of the total torque imparted to the envelope and each base of the particle. By order of magnitude conside-rations (APPENDIX 2), it can be shown that the ordinary translational velocity of an aerosol particle, U_M , is negligible with respect to v_2 and $\omega \times R$ (Eq. [44]). Consequently, it becomes possible to express the integrand of [44] for the molecules which hit the particles envelope, for example, as

$$I_1 = i \cdot [\, R \times (v_2 - \omega \times R)][(v_2 - \omega \times R) \cdot n\,] = -\, z \sin\phi \, v_2^{s\,2}$$

$$+\, (-\, \omega_1 z^2 - \omega_1 \varsigma^2 \sin^2\phi - \omega_1 z^2 \sin^2\phi + \omega_2 \varsigma^2 \cos\phi \sin\phi + \omega_2 z^2 \cos\phi \sin\phi$$

$$+\, \omega_3 \varsigma z \cos\phi)\, v_2^{s} + (\omega_1 \varsigma z \sin^2\phi - \omega_2 \varsigma z \sin\phi \cos\phi)\, v_2^{z} + (-\, \omega_1 z^2 \sin\phi \cos\phi$$

$$+\, \omega_2 z^2 \cos^2\phi)\, v_2^{\phi} + \varsigma \sin\phi \, v_2^{s} v_2^{z} - z \cos\phi \, v_2^{s} v_2^{\phi} - \omega_1^2 z^3 \sin\phi$$

$$+\, \omega_1^2 \varsigma^2 z \cos^2\phi \sin\phi - \omega_2^2 \varsigma^2 z \cos^2\phi \sin\phi - \omega_1^2 \varsigma^2 z \sin\phi + 2\,\omega_1 \omega_2 \varsigma^2 z$$

$$\cos\phi \sin^2\phi + \omega_1 \omega_2 z^3 \cos\phi + \omega_1 \omega_3 \varsigma z^2 \cos\phi \sin\phi - \omega_2 \omega_3 \varsigma z^2$$

$$\cos^2\phi \; . \tag{63}$$

The integration limits in the (governing equation) [44] are set to be

$$-\infty \leq v_1 \cdot n = v_2^{s} + \omega_1 z \sin\phi - \omega_2 z \cos\phi \leq 0 \; , \quad \text{which leads to}$$

$$-\infty \leq v_2^{s} \leq \omega_2 z \cos\phi - \omega_1 z \sin\phi \; ,$$

and

$$-\infty \leq v_2^{\phi}, \; v_2^{z} \leq \infty \qquad .$$

Finallly, in this case, the torque can be written in the form

$$(L_F \cdot i)_c^{(in)} = -\, N m \, (h/\pi)^{3/2} \iint_{S_c} \int_{v^z} \int_{v^\phi} \int_{v^s} I_1 \; e^{-h(v_2^{s\,2} + v_2^{\phi\,2} + v_2^{z\,2})}$$

$$d v_2^{s} \, d v_2^{\phi} \, d v_2^{z} \, d S \tag{64}$$

where the velocity limits are given by the above, and $d S = \varsigma \, d z \, d\phi$

$$(\, 0 \leq \phi \leq 2\pi \, , \; -\tfrac{L}{2} \leq z \leq \tfrac{L}{2} \,) \; .$$

For the case of $h^{1/2} \omega_i z \ll 1$ which almost always occurs (APPENDIX 2), and when utilizing certain integral values (APPENDIX 2), one obtains in the typical procedure shown here that

$$
\left(L_F \cdot i \right)_c^{(in)} = - N m \langle h / \pi \rangle^{1/2} \int [- \frac{\pi^{1/2} z \sin\phi}{4 \, h^{3/2}} - \frac{1}{2h} (- \omega_1 \varsigma^2 \sin^2\phi
$$

$$
- \omega_1 z^2 \cos^2\phi + \omega_2 \varsigma^2 \cos\phi \sin\phi - \omega_2 z^2 \cos^2\phi \sin\phi + \omega_3 \varsigma z \cos\phi)
$$

$$
+ (\omega_1^2 \varsigma^2 z \cos^2\phi \sin\phi + \omega_1^2 \varsigma^2 z \sin\phi - \omega_1^2 z^3 \sin\phi - \omega_2^2 \varsigma^2 z \cos^2\phi \sin\phi
$$

$$
+ \omega_1 \omega_2 z^3 \cos\phi + \omega_1 \omega_2 \varsigma^2 z \sin^2\phi + \omega_1 \omega_2 \varsigma^2 z \cos\phi \sin^2\phi + \omega_1 \omega_3 \varsigma z^2
$$

$$
\cos\phi \sin\phi - \omega_2 \omega_3 \varsigma z^2 \cos^2\phi) (\frac{1}{2} (\frac{\pi}{h})^{1/2} + \omega_2 z \cos\phi - \omega_1 z \sin\phi) + 0(\cdots)] d\varsigma \quad [65]
$$

where $0(\ldots)$ denotes higher powers of $\omega_i \, \omega_j$ which can be neglected (APPENDIX 2).

II. Results

1. The Spherical Particle

The total torque on the spherical particle for $\omega = \omega k$ and is found to be

$$
\left(L_F \cdot k \right)^{(tot)} = - \alpha (\frac{\pi}{h})^{1/2} \omega N m r^4 (\frac{4}{3} + \frac{8}{15} h \, U_H^2) \quad [66]
$$

which, for the common case of $\qquad h^{1/2} U_M \ll 1 \qquad$ (APPENDIX 2), turns to

$$(L_F \cdot k)^{(tot)} = \alpha \, (4/3) \, (\pi/h)^{1/2} \, \omega \, N \, m \, r^4 \; . \qquad [67]$$

Eq. [67] is <u>exactly</u> similar to that obtained by Epstein (18) in a different way and so one may certainly have confidence in the calculational method.

It should be remarked that in the above case

$$(L_F \cdot i)^{(tot)} = (L_F \cdot j)^{(tot)} = 0 \qquad\qquad [68]$$

as can be easily seen.

For the arbitrary U_M direction, it is found that

$$(L_F \cdot k)^{(tot)} = \alpha \, (\pi/h)^{1/2} \, \omega \, N \, m \, r^4$$

$$\times \left[\frac{4}{3} + \frac{8}{15} \, (1 + \sin^2\Psi) \, h \, U_M^2 \right] \qquad [69]$$

which becomes identical with [66] as $\Psi = 0$.

2. The Cylindrical or Discoidal Particle

The total torque on these particles is

$$(L_F \cdot i)^{(tot)} = -\left(\frac{\pi}{h}\right)^{1/2} \omega_1 \, N \, m \, \varsigma \, L^3 \left[\left(\frac{1}{4} + \frac{1}{2}\beta + \beta^2 + \beta^3\right) \right.$$

$$+ \alpha \left(\frac{\pi-6}{48} - \frac{1}{4}\beta - \frac{1}{2}\beta^2 + \frac{\pi-4}{8}\beta^3\right) + \frac{\pi^{1/2} h^{1/2} \omega_2 \omega_3}{4\omega_1} \left(\frac{\varsigma^3}{L^2}\right.$$

$$\left. - \frac{\varsigma}{3}\right) + \alpha \left[\frac{\pi^{1/2} h^{1/2} \omega_2 \omega_3}{8\omega_1} \left(\frac{\varsigma}{3} - \frac{\varsigma^3}{L^2}\right) + h\left(\omega_1^2 + \omega_2^2\right) \right.$$

$$\left. \left(\frac{\varsigma^2}{16} + \frac{L^2}{80} - \frac{\varsigma^3}{8L} + \frac{\varsigma^5}{4L^3}\right)\right] + O(\cdots) \qquad [70]$$

which can be written to a very good approximation (APPENDIX 2) as

$$(L_F \cdot i)^{tot} \cong -\left(\frac{\pi}{h}\right)^{1/2} \omega_1 \, N \, m \, \varsigma \, L^3 \left[\left(\frac{1}{4} + \frac{1}{2}\beta + \beta^2 + \beta^3\right) \right.$$

$$\left. + \alpha \left(\frac{\pi-6}{48} - \frac{1}{4}\beta - \frac{1}{2}\beta^2 + \frac{\pi-4}{8}\beta^3\right)\right] \qquad [71]$$

where $\quad \beta = \varsigma / L \quad .$

Similarly to Eq. 71 , it is possible to get an equation for the torques imparted to the rotating aerosol particle along its other axes; these come out to be

$$(L_F \cdot j)^{(tot)} \sim -\omega_2 \qquad [72]$$

and

$$(L_F \cdot k)^{(tot)} \sim -\omega_3 \quad . \qquad [73]$$

Thus, the (vector) torque can be written as

$$L_F = -\Omega \cdot \omega \qquad [74]$$

where $\Omega = \overset{r}{M}^{-1}$ is a <u>symmetric</u> diadic whose eigenvectors lie along the symmetry axes of the particle. A similar deduction can be reached from Landau's and Lifshitz's (19) reasoning based on irreversible thermodynamics principles.

a. The rotational diffusion coefficient

From Eq. [38] one has that

$$\overset{r}{D}_\perp = -\frac{\omega_1}{(L_F \cdot i)^{(tot)}} kT \qquad [75]$$

which gives, if one uses the kinetic theory relationship $Nm(\frac{\pi}{h})^{1/2} = \mu (\pi/\bar{l})$

$$\overset{r}{D}_\perp = \frac{kT \ Kn}{\pi \mu L^3 \left[(\frac{1}{4} + \frac{1}{2}\beta + \beta^2 + \beta^3) + \alpha(\frac{\pi-6}{48} - \frac{1}{4}\beta - \frac{1}{2}\beta^2 + \frac{\pi-4}{8}\beta^3) \right]} \qquad [76]$$

where $Kn = \bar{l}/\varsigma$.

Eq. [76] should be compared to that of Edwards (20)

$$\overset{r}{D}_\perp^E = \frac{kT}{8\pi\mu (L^3/3)(\frac{1}{0.1931 + \ln\beta})} \qquad [77]$$

as is presented in Fig. 25.
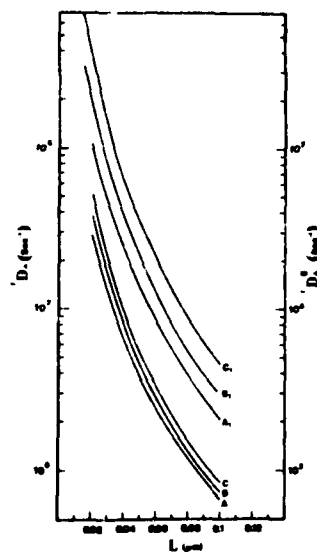
Fig. 25. The rotational diffusion coefficient of Cylindrical
particles in air. A_1, B_1, C_1 - values of this study;
A,B,C - Edwards' values.

III. Discussion

It must be re-noted here that our calculations apply to aerosol
particles whose dimension, in any direction, is much smaller than the
mean-free path $\bar{l}$ of the gas molecules (≈ 0.069 μm at normal conditions),
and to a quiet medium. For larger particles within a flow, one has to
recur to the Boltzmann's integro-differential equation of the velocity
distribution whose (closed form) solution is not known as yet.

The results of $^r D_\perp$ themselves show that:

i. The values of the coefficient are of the order of 10^6-10^7 sec^{-1}, which makes the typical relaxation times for Brownian rotation phenomenta, $\tau_r = 1/\perp_-$ negligibly small.

ii. The calculated values are greater by a factor of about 30 than those obtained according to Edwards in classical fluiddynamic means, which is reflected by the rotational Peclet number assigned to a diffusional condition of orientable particles and, hence, by the orientational distribution density.

IV. Applications

As an example for the use of $^r D_\perp$ in a real problem, it is possible to take the diffusional deposition of cylindrical aerosol particles on an infinite plannar surface and in a quiet medium.

a. General

Employing the cartesian coordinate system shown in Fig. 26, one can write down Eq. [27] in the form

$$\frac{\partial \sigma}{\partial t} = [^t D_\perp + (^t D_{\parallel} - ^t D_\perp) \sin^2\theta \cos^2\phi] \frac{\partial^2 \sigma}{\partial x_1^2} + [^t D_\perp + (^t D_{\parallel} - ^t D_\perp)$$

$$\sin^2\theta \sin^2\phi] \frac{\partial^2 \sigma}{\partial x_2^2} + [^t D_\perp + (^t D_{\parallel} - ^t D_\perp) \cos^2\theta] \frac{\partial^2 \sigma}{\partial x_3^2}$$

$$+ 2(^t D_{\parallel} - ^t D_\perp)[\sin^2\theta \sin\phi \cos\phi \frac{\partial^2 \sigma}{\partial x_1 \partial x_2} + \sin\theta \cos\theta \sin\phi$$

$$\frac{\partial^2 \sigma}{\partial x_2 \partial x_3} + \sin\theta \cos\theta \cos\phi \frac{\partial^2 \sigma}{\partial x_1 \partial x_3}] + ^r D_\perp [\frac{1}{\sin\theta} \frac{\partial}{\partial \theta}(\sin\theta \frac{\partial \sigma}{\partial \theta} + \frac{1}{\sin^2\theta} \frac{\partial \sigma}{\partial \phi^2}] \qquad [78]$$

Fig. 26. The cartesian system of coordinates used in the
diffusion analysis.

where $\overset{t}{D}_{\parallel}$, $\overset{t}{D}_{\perp}$ are the __translational__ diffusion coefficients of the
particle parallel and perpendicular to its polar axis, respectively. Now,
if it is assumed that particles' orientation density is independent of
their location viz.

$$\sigma(r, \phi, t) = c(x_1, x_2, x_3) f(\theta, \phi, t) ,$$ [79]

then, instead of [78] , one obtains the two equations:

$$\partial f / \partial t = \overset{r}{D}_{\perp} \left[\frac{1}{\sin\theta} \frac{\partial}{\partial\theta} \left(\sin\theta \frac{\partial f}{\partial\theta} \right) + \frac{1}{\sin^2\theta} \frac{\partial^2 f}{\partial\phi^2} \right]$$ [80]

whose solution is given in Eq. [35] , and

$$\frac{\partial c}{\partial t} = [\ ^t D_\perp + (\ ^t D_{\shortparallel} - \ ^t D_\perp)\ sin^2\theta\ cos^2\phi]\ \frac{\partial^2 c}{\partial x_1^2} + [\ ^t D_\perp + (\ ^t D_{\shortparallel} - \ ^t D_\perp)$$

$$sin^2\theta\ sin^2\phi]\ \frac{\partial^2 c}{\partial x_2^2} + [\ ^t D_\perp + (\ ^t D_{\shortparallel} - \ ^t D_\perp)\ cos^2\theta]\ \frac{\partial^2 c}{\partial x_3^2}$$

$$+ 2(\ ^t D_{\shortparallel} - \ ^t D_\perp)[\ sin^2\theta\ sin\phi\ cos^2\phi\ \frac{\partial^2 c}{\partial x_1\ \partial x_2} + sin\theta\ cos\theta\ sin\phi$$

$$\frac{\partial^2 c}{\partial x_2\ \partial x_3} + sin\theta\ cos\theta\ cos\phi\ \frac{\partial^2 c}{\partial x_3\ \partial x_1}\ ]\ . \tag{81}$$

At this stage, the orientation averaging being defined by

$$\langle g \rangle \qquad \frac{\int_0^{2\pi}\int_0^\pi g\ f(\theta, \phi, t)\ sin\theta\ d\theta\ d\phi}{\int_0^{2\pi}\int_0^\pi f(\theta, \phi, t)\ sin\theta\ d\theta\ d\phi} \quad ,$$

one reaches the final equation

$$\left\langle \frac{\partial c}{\partial t} \right\rangle = \frac{\int_0^{2\pi}\int_0^\pi \frac{\partial c}{\partial t}\ f(\theta, \phi, t)\ sin\theta\ d\theta\ d\phi}{\int_0^{2\pi}\int_0^\pi f(\theta, \phi, t)\ sin\theta\ d\theta\ d\phi} = \frac{\partial c}{\partial t}$$

$$= [\ ^t D_\perp + (\ ^t D_{\shortparallel} - \ ^t D_\perp)\langle sin^2\theta\ cos^2\phi \rangle]\ \frac{\partial^2 c}{\partial x_1^2} + [\ ^t D_\perp + (\ ^t D_{\shortparallel} - \ ^t D_\perp)$$

$$\langle sin^2\theta\ sin^2\phi \rangle]\ \frac{\partial^2 c}{\partial x_2^2} + [\ ^t D_\perp + (\ ^t D_\perp + (\ ^t D_{\shortparallel} - \ ^t D_\perp)\langle cos^2\theta \rangle)]\ \frac{\partial^2 c}{\partial x_3^2} \tag{82}$$

since the mixed terms $\partial^2 c\ /\ \partial x_i\ \partial x_j$ drop out.

b. Specific

In the specific, above diffusion case where it is taken that concentration gradients exist only along x_2

$$\frac{\partial c}{\partial t} = \mathcal{D}(t)\ \frac{\partial^2 c}{\partial x_2^2} \tag{83}$$

where the orientation-averaged translational diffusion coefficient $\mathscr{D}(t)$

is

$$\mathscr{D}(t) = {}^t D_\perp + ({}^t D_{\parallel} - {}^t D_\perp) \langle \sin^2 \theta \sin^2 \phi \rangle \quad . \qquad [84]$$

Peforming the orientation-averaging of the function $\sin^2 \theta \sin^2 \phi$ one gets that

$$\mathscr{D}(t) = {}^t D_\perp + ({}^t D_{\parallel} - {}^t D_\perp) \left\{ \frac{1}{3} [1 - exp(-6 \, {}^r D_\perp t)] \right\} . \qquad [85]$$

Concerning the solution of [83] , it is advantageous to define a (new) vriable P by (21)

$$P = \int_0^t \mathscr{D}(t') \, dt' \qquad [86]$$

whereby one obtains that (for $c = c_0$ at $t = 0$ and $c = 0$ at $x_2 = 0$ and $t > 0$)

$$c = c_0 \, \Phi \left(\frac{x_2}{2 \, P^{1/2}} \right) = c_0 \, \Phi \left[\frac{x_2}{2 \left(\int_0^t \mathscr{D}(t') \, dt' \right)^{1/2}} \right] , \qquad [87]$$

Φ being the Error Function.

The total number of deposited particles M_t after time t will be then (22)

$$M_+ = 2 c_0 \left(\frac{\int_0^t \mathscr{D}(t') dt'}{\pi} \right)^{1/2} . \qquad [88]$$

c. Results

The number M_T vs. time is presented in Fig. 27 for the two cases:

A. When $^{+}D_{\parallel}$ and $^{+}D_{\perp}$ are calculated according to classical continuum theory, viz.

$$^{+}D_{\parallel} = \frac{kT}{2 \pi \mu L \left[1/\langle \ln (1/\beta) - 0.5 \rangle \right]} \qquad [89]$$

and

$$^{+}D_{\perp} = \frac{kT}{4 \pi \mu L \left[1/\langle \ln (1/\beta) + 0.5 \rangle \right]} \qquad [90]$$

and Edwards' value of $^{r}D_{\perp} (\equiv {}^{r}D_{\perp}^{E})$ is assumed.

B. When these coefficients are given by Dahneke's molecular regime equations, viz.

$$^{+}D_{\parallel} = \frac{kT \, Kn}{\pi \mu \, S \left[4 + \alpha \langle 1 + (1/\beta) - (6-\pi)/4 \rangle \right]} \qquad [91]$$

and

$$^{+}D_{\perp} = \frac{kT \, Kn}{\pi \mu \, S \left[(2/\beta) + \alpha \langle 1 + (1/\beta) - (6-\pi)/4 \rangle \right]} \qquad [92]$$

and our value of $^{r}D_{\perp}$ is taken.

Also, M_t is calcuaited for case C of a volumetrically equivalent spherical particle.

From Fig. 27 it is seen that the values of case B are significantly higher than those of case A but that those of case C are higher still, which is resonable if one remembers that diffusional particle mobility is a property of the surface of the latter and that the surface of the volumetrically equivalent sphere is the smallest of all forms.

It should be noted that in the still-medium diffusion discussed here is essentially independent of the (very large) value of $\mathcal{D}(t)$ for all experimental times of interest. The value of $^r D_\perp$ will matter in difusion in flow where the rotational Peclet number $^r Pe_\rho$ $(= |\omega| / ^r D_\perp)$ does count.

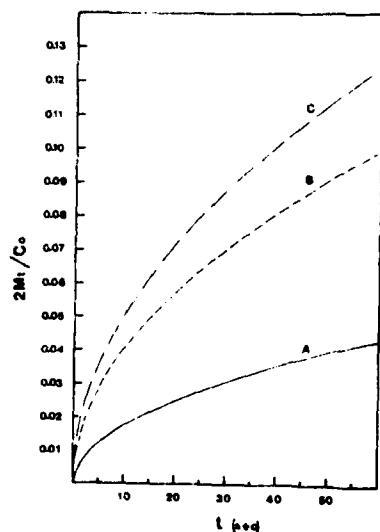Fig. 27. The total number M_t vs. t.

A, case A; B, case B ; C, case C cited above .

$\wp = 0.0075 \mu m$, $L = 0.1 \mu m$, $T = 298.16 \,^\circ K$, $\mu = 184.22 \times 10^{-6}$ poise,

$\bar{l} = 6.69 \times 10^{-6} cm$.

C. APPENDIX 1,2

1. Appendix 1

   a. Green functions

   Generally, expressing the disturbance due to the slender body
by (Fig. 1)

$$v_i(r) + V_i^{(2)}(r) = \int_s u_{ij}(r, r'') \, f_j(r'') \, dr'' \qquad [C.1]$$

where $f_j(r'')$ is the drag force <u>per unit surface</u> and $V_i^{(2)}(r)$
is the double-layer potential (which can be neglected), and using the
radius vector r' (Fig.1) to define position, one can expand $u_{ij}(r,r'')$
according to

$$u_{ij}(r, r'') = u_{ij}(r, r') + s_k'\left(\frac{\partial}{\partial r'_k}\right) u_{ijk}$$

$$+ \frac{1}{2} s_k' s_\lambda' \left(\frac{\partial^2}{\partial r'_k \partial r'_\lambda}\right) u_{ijk\lambda} + \cdots$$

where $\rho'(r', \varphi)$ is the radial vector of the point $P'(r'')$
starting from its vertical projection on the axis. Then, one can write

$$v_i(r) = \int_{-l}^{l} f_j(r') \, u_{ij}(r, r') \, dr' + \int_{-l}^{l} f_{jk}(r') \, u_{ijk}(r, r') \, dr' + \cdots \quad [C.2]$$

where

$$f_j(r') = \oint s' f'_j(r', s') \, d\varphi \; ,$$

$$f_{jk}(r') = \oint s' s_{k'} f'_j(r', s') \, d\varphi \qquad \text{etc.}$$

since

$$r'' = r' + s'(r', \varphi) \; .$$

b. Definitions

$$C_1 = C'_1 \cos\theta + C'_2 \sin\theta \, , \; C_2 = -C'_1 \sin\theta + C'_2 \cos\theta \, , \; C_3 = C'_3 \; .$$

$$M_{11} = 2\cos^2\theta + \sin^2\theta \, , \; M_{12} = M_{21} = -\sin\theta\cos\theta \, , \; M_{13} = M_{31} = 0 \, ,$$

$$M_{22} = 2\sin^2\theta + \cos^2\theta \, , \; M_{23} = M_{32} = 0 \, , \; M_{33} = 1 \; .$$

$$\pi_{11} = K\cos^2\theta + K_{22}\sin^2\theta \, , \; \pi_{12} = \pi_{21} = (K_{22}-K)\sin\theta\cos\theta \, ,$$

$$\pi_{13} = K_{23}\sin\theta \, ; \; \pi_{22} = K\sin^2\theta + K_{22}\cos^2\theta \, , \; \pi_{23} = K_{23}\cos\theta \, ,$$

$$\pi_{31} = K_{32}\sin\theta \, , \; \pi_{32} = K_{32}\cos\theta \, , \; \pi_{33} = K_{33} \; .$$

$$I_{11} = (s_2^2/s^2)\sin^2\theta \, , \; I_{12} = I_{21} = (s_2^2/s^2)\sin\theta\cos\theta \, ,$$

$$I_{13} = I_{31} = (s_2 s_3/s^2)\sin\theta \, , \; I_{22} = s_2^2\cos^2\theta \, , \; I_{33} = (s_3^2/s^2) \; .$$

$$I'_{11} = \sin\theta \, , \; I'_{12} = I'_{21} = \sin\theta\cos\theta \, , \; I'_{13} = 0 \, , \; I'_{22} = \cos^2\theta \, ,$$

$$I'_{23} = I'_{32} = I'_{31} = 0 \; .$$

$$I''_{11} = \cos^2\theta \, , \; I''_{12} = I''_{21} = -\sin\theta\cos\theta \, , \; I''_{22} = -\sin\theta \, , \; I''_{13} = I''_{31} = 0 \; .$$

where θ is the angle between x_i and $x_{i'}$.

$$\gamma_{\ell}(s) = \int_{-\ell}^{\ell} -\frac{f_\ell(s) - f_\ell(r')}{|s - r'|} \, dr' ;$$

$$\Lambda_i(r) = \int_{-\ell}^{\ell} f_j(r') \, \omega_{ij}(r, r') \, dr' .$$

c. Elaborate procedure

This procedure is based on Eq. [20]. Employing the transformations:

$$x \longrightarrow x_n = n\Delta , \quad x' \longrightarrow x_{n'} = n'\Delta \quad \text{where } \Delta = 2\ell/N ,$$

one defines

$$F(n, n') = \Delta(n - n') , \quad r_1^*(n, n') = \cos\theta \, (n - n') , \quad r_2^*(n, n') = 0 ,$$

$$r_3^*(n, n') = \sin\theta \, (n - n')\Delta , \quad r_1(n, n') = \cos\theta \, (n - n')\Delta ,$$

$$r_2(n, n') = 0 , \quad r_3(n, n') = \sin\theta \, (n - n')\Delta , \quad h(n, n') = n'\Delta + \mathcal{D} ,$$

$$M'_{ij}(n, n') = M_{ij}\, \ln \frac{(n' - n + 0.5)\,\Delta}{(n' - n - 0.5)\,\Delta} \quad \text{if} \quad n > n' ,$$

$$M'_{ij}(n, n') = M_{ij}\, \ln \frac{(n' - n + 0.5)\,\Delta}{(n' - n - 0.5)\,\Delta} \quad \text{if} \quad n < n'$$

and writes   [17]   and   [18]   in terms of these transformations.

Thus, $u_{ij}^w (x,x') \longrightarrow \Lambda_{ij} (n,n')$ and Eq. [20] is expressed as

$$U'(\gamma) = \sum_{\gamma'} T(\gamma,\gamma') f_{\gamma'}$$

where $\gamma = N(i-1) + n$, $\gamma' = N(j-1) + n'$, $T(\gamma,\gamma')$

$$= \frac{1}{2} M(\gamma,\gamma') + \Lambda(\gamma,\gamma') \text{ for } \gamma \neq \gamma' , \quad T(\gamma,\gamma') = N(\gamma,\gamma') + \Lambda'(\gamma,\gamma') \text{ for } \gamma = \gamma'.$$

2. Appendix 2

a. Order of magnitude of $h^{1/2} U_M$

Taking a typical case of $U_M = O(1)$ and calculating h to be

5.47×10^{-10} $sec^2 cm^{-2}$ for $T = 298.16 °K$ and air molecules,

one obtains that

$$h^{1/2} U_M = O(10^{-5}), \text{ which is much smaller}$$

than unity.

b. Order of magnitude of $h^{1/2} r_o \omega_i$

Taking $L = 0.1 \times 10^{-4} cm$, $g = 0.0075 \times 10^{-4} cm$, $g_p = 1 g. cm^{-5}$

and air molecules at $T = 298.16 °K$, $\mu = 184.22 \times 10^{-4} poise, \bar{l} = 6.69 \times 10^{-6} cm$.,

and estimating ω_i by the law of equipartition of energy, viz.

$$\frac{1}{2} I_i \langle \omega_i^2 \rangle = \frac{1}{2} kT ,$$ [C.3]

one gets that

$$h^{1/2} g \langle c_1^2 \rangle^{1/2} = 2.91 \times 10^{-4}$$

and

$$h^{1/2} \langle x_1^2 \rangle^{1/2} = 3.87 \times 10^{-3} \; .$$

d. Integrals

$$\int_{-\infty}^{\pm g} x^2 e^{-hx^2} dx = \frac{\pi^{1/2}}{4 h^{3/2}} \left[1 \pm \Phi(h^{1/2} g)\right] \mp \frac{1}{2h} g\, e^{-hg^2}$$

$$\int_{-\infty}^{\pm g} x\, e^{-hx^2} dx = \frac{-e^{-hg^2}}{2h} \quad ,$$

$$\int_{-\infty}^{\pm g} e^{-hx^2} dx = \frac{\pi^{1/2}}{2 h^{1/2}} \left[1 + \Phi(h^{1/2} g)\right] \; ,$$

$$\int_{-\infty}^{\infty} e^{-hx^2} dx = (\pi/h)^{1/2} \quad ,$$

$$\int_{-\infty}^{\infty} x\, e^{-hx^2} dx = 0 \quad ,$$

$$\int_{-\infty}^{\infty} x^2 e^{-hx^2} dx = \frac{\pi^{1/2}}{2 h^{3/2}} \; .$$

D. NOMENCLATURE

a - constant of systems geometry; half-width of flow channel

A,B - transformation matrices defined in text

b-   characteristic equivalent cross-section radius of (slender) particle

b_r-   local equivalent cross-section radius

B_i , $B_i^{(i)}$, B_i^{ii} , B_i - constants

c -   particles' total number concentration, o - initial value

C -   vector, defined in text

D -   distance, defined in Fig. 2

^tD , ^rD , ^cD - translational, rotational and coupling diffusion diadics, respectively

$^rD_\perp$ - rotational diffusion coefficient around a mid-diameter

$^tD_{||}$, $^t_\perp$ - translational diffusion diadic components parallel and perpendicular to polar axis, respectively

D_1 , D_2 - distances, defined in Fig.4

$\mathscr{D}$ - $^tD_\perp + (^tD_{||} - ^tD_\perp)\langle \sin^2\theta \, \sin^2\phi \rangle$

e   - unit vector along symmetry axis of particle

f   - orientation distribution density

$f_i(r')$ - Stokeslets' distribution density; $f_{jk}(r)$ -doublets' distribution density etc.

$f_i(r''$ - drag force per unit area of particle

F_e - external force; F_F - fluiddynamic force

g   - acceleration of gravity

h   - particle-wall distance; also, m/2kT

I^* , I_i - moment of inertia of particle

I , I', I" - diadics, defined in text

I_i - intergrand, defined in text

$\mathscr{j}$ - rotational flux of axi-symmetric particles

J   - particles' flux

|J| - transformation Jacobian

k   - Boltzmanns constant

k_1 , k_2- constants

Kn   - Knudsen's number

l   - semi-length of slender particle

$\bar{l}$ - mean free- path of gas molecules

L   - length of cylindrical particle

ℓ   - external torque; ℓ   - fluiddynamic torque

m	- mass of particle
M_t	- total number of deposited particles in time t
M	- diadic, defined in text
$\overset{\infty}{M}$	- mobility diadic
π	- unit vector normal to dS
n, n'	- running indices
ν', ν, ν_v	- number of molecules hitting unit surface per unit time
ν_{v_2}	- density of Maxwell's velocity distribution
N	- average number of gas molecules
P	- defined in text
P_r	- rotational Peclet number
^rPe_f	- particle rotational Peclet number
P_n^m	- associated Legendre function
r_c	- typical length of particle
r, r', r'', r^*	- distances defined in Fig. 1 and 2
r	- location radius vector , r - radius of sphere
R	- radius vector from geometric center of particle to a point on its surface.
S	- particles surface; dS - surface element
t	- time
T	- Temperature
$u_{ij}(r, r')$ -	etc. - Green functions associated with
U_M, u	- translational velocity of particle
$v(r)$	- disturbance velocity of slender body
v_2, v_1	- velocities of gas molecules in the O_2 system and relative to dS respectively; v' - velocity of reflected molecules.
V	- translational velocity of slender body
$V^{(2)}(r)$	- double-layer potential
X, x'	- position distances on body's axis (Fig.1)
X_1, X_2, X_3	- coordinates

Greek letters

α - fraction of gas molecules reflected diffusely

β - ϱ

$\;$ - running indices

δ - Kronickers' delta

Δ - $1/N$

ϵ - Levi-Civita permulation tensor

ζ - fluid's vorticity

η - angle, defined in text

θ,ϕ - polar angles

Λ - vector, defined in text

μ - dynamic viscosity of gas

π - diadic, defined in text

ξ - position vector, defined in Fig. 1

ρ - gas density; cylinder's radius

ρ_o - particles' density

σ - number concentration in location-orientation hyper-space;

$\qquad$ also, $\left[\ell_n\left(2l/s\right)\right]^{-1}$

ϕ - orientation (pseudo)vector

Φ - Error Function

Ψ - angle between U_M and ω

ω - rotational velocity of particles; ω_1, ω_2, ω_3 -components

$\Omega \quad = \; r_M^{-1}$

Subscripts

M - center of mass

o - initial value

c - cylinder's envelope

Superscripts

(in) - hitting molecules

α - t,r,c

(r)   - reflected molecules

(tot) - total

E. REFERENCES

1. Brenner, H., Chem.Eng. Sci. 16, 242 (1961).

2. Gallily, I. and Mahrer, Y., J. Aerosol Sci. 4, 253 (1973.

3. Wakiya, S., Res. Rep. Fac.Emg. Niigata Univ.(Japan) 8, 17, (1959).

4. Oberbeck, H.A. , Crelles J. 81, 79 (1876).

5. Jeffery, G.B., Proc. Roy.Soc.London 102A, 161 (1923).

6. Batchelor, G.K., J. Fluid Mech. 44, 419 (1970).

7. Chwang, A.T. ibid, 72, 17 (1975).

8. Blake, J.R.,ibid., J.Eng. Math. 8, 313 (1974).

9. Cox, R.G., ibid., 44, 791 (1970).

10. Kerker,M.,"The Scattering of Light",Academic Press, New York,1969,Chap.6.

11. Wang, C.S., Seaborg, J.J. and Lin, S.P., Phys.Fluids 21, 2365 (1978).

12. Happel, J. and Brenner,H. "Low Reynolds Number Hydrodynamics" Prentice-Hall, N.J., 1965, p. 187.

13. Gallily, I., Holländer,W. and Stoeber, W., "The Separation of Nonspherical Aerosol particles from Bojndary Flows", Final Report to DFG (Germany), 1981.

14. Brenner, H. and Condiff, D.W., J. Colloid Interface Sci. 41, 228 (1972); 47, 199 (1974).

15. Vadas, E.B., Cox, R.G., Goldsmith, H.L. and Mason, S.G.,ibid, 57, 308 (1976).

16. Peterlin, A., Z.Physik 111, 232 (1938).

17. Brenner, H., J. Colloid Interface Sci. 23, 407 (1967).

18. Epstein, P., Phys.Rev.23, 710 (1924).

19. Landau, L.D. and Lifshitz, E.M., "Mechanico, Pergamon,1960, p. 76.

20. Edwards, D., in Gans R., Ann Physik (Leipzig) 86, 628 (1928).

21. Crank, J., "The Mathematics of Diffusion", Oxford Univ. Press. (Clarendon) London/New York, 1956, p. 147.

22. ibid, p. 31.

23. Dahneke, B.E., J. Aerosol Sci. 4, 147 (1971).